Aalto University

CHEM-E5140
Materials Characterization

TEM Lecture
23.09.2020

Yanling Ge
Yanling.ge@aalto.fi
Yanling.ge@vtt.fi

TEM

- Transmission Electron Microscope
  - Illumination system – gun + condenser
  - Specimen stage
  - Imaging system – objective + projector
- TEM application – Diffraction
- TEM Imaging Contrast and HRTEM
- Specimen preparation

Transmission Electron Microscope

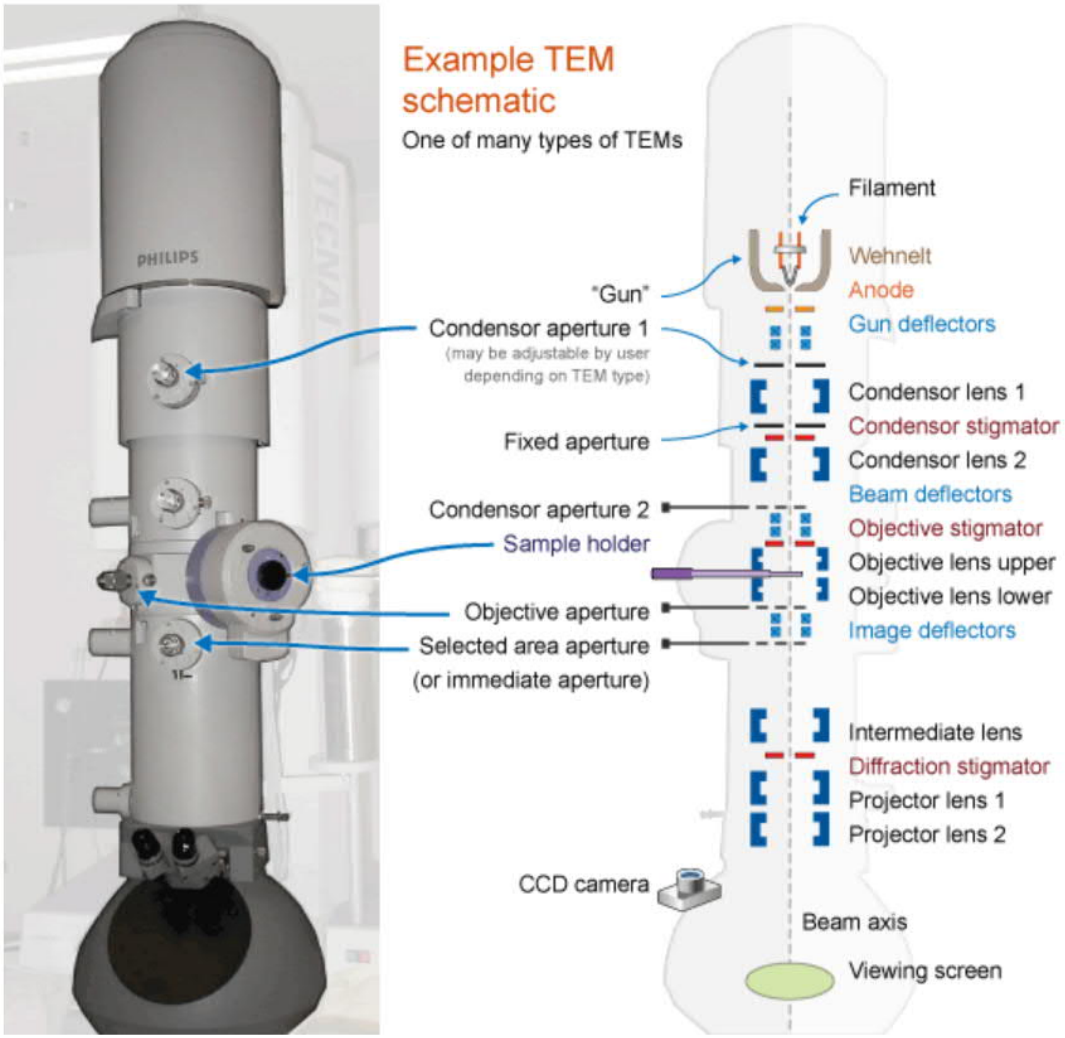

A generalised cut-away diagram of the internal structure of a transmission electron microscope alongside an example of a modern instrument.

https://www.ammrf.org.au/myscope/tem/introduction/

Electron gun - Thermionic vs Field emission gun

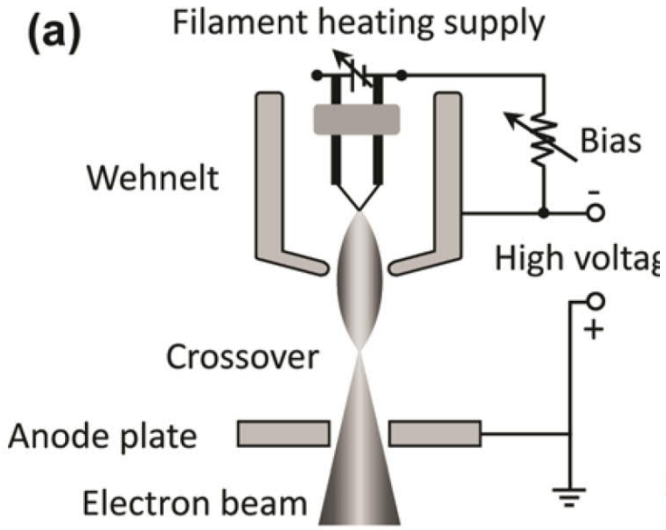

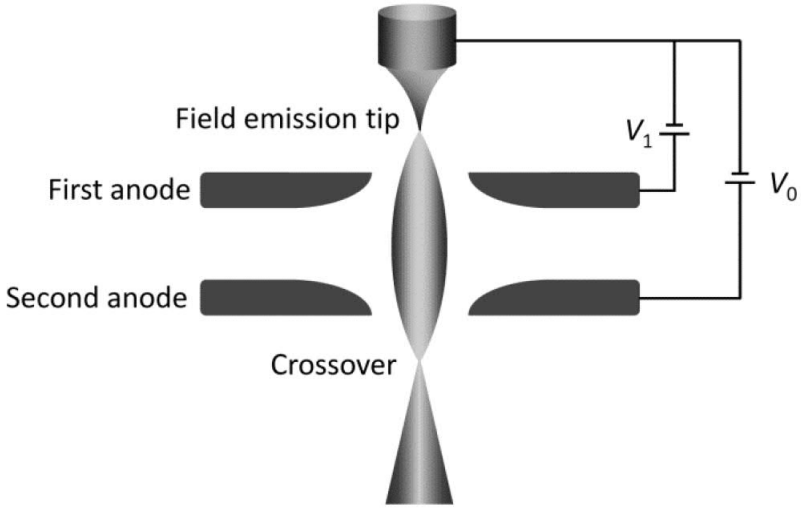

Fig. 3.3 Construction of FEG. V_1 is the extraction voltage, and V_0 is the acceleration voltage.

FEG has higher current density!

TABLE 5.1 Characteristics of the Principal Electron Sources

	Units	Tungsten	LaB_6	Schottky FEG	Cold FEG
Work function, Φ	eV	4.5	2.4	3.0	4.5
Richardson's constant	A/m^2K^2	6×10^9	4×10^9		
Operating temperature	K	2700	1700	1700	300
Current density (at 100 kV)	A/m^2	5	10^2	10^5	10^6
Crossover size	nm	$> 10^5$	10^4	15	3
Brightness (at 100 kV)	A/m^2sr	10^{10}	5×10^{11}	5×10^{12}	10^{13}
Energy spread (at 100 kV)	eV	3	1.5	0.7	0.3
Emission current stability	%/hr	<1	<1	<1	5
Vacuum	Pa	10^{-2}	10^{-4}	10^{-6}	10^{-9}
Lifetime	hr	100	1000	>5000	>5000

Electromagnetic lens (convex lens)

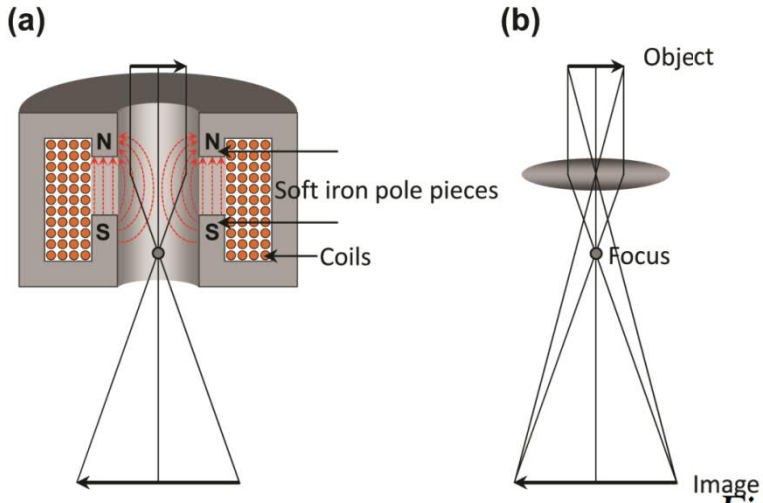

Fig. 3.4 (a) Electromagnetic lens; (b) optical lens.

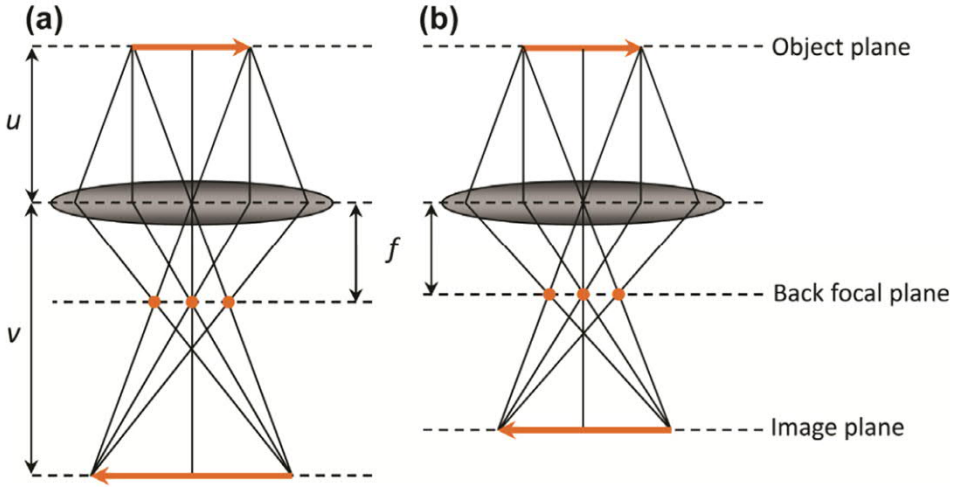

Fig. 3.5 Relationship between object distance u, image distance v and focal length f. (a, b) u remains the same, while f is changed.

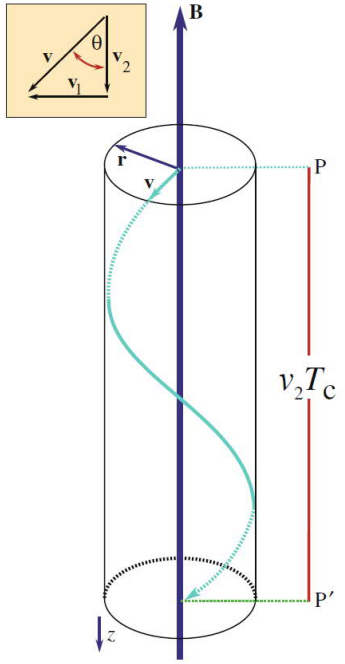

$$\frac{1}{f} = \frac{1}{u} + \frac{1}{v} \qquad M = \frac{v}{u}$$

$$F = evB\sin\theta = evB = \frac{mv^2}{r}$$

Electromagnetic lens

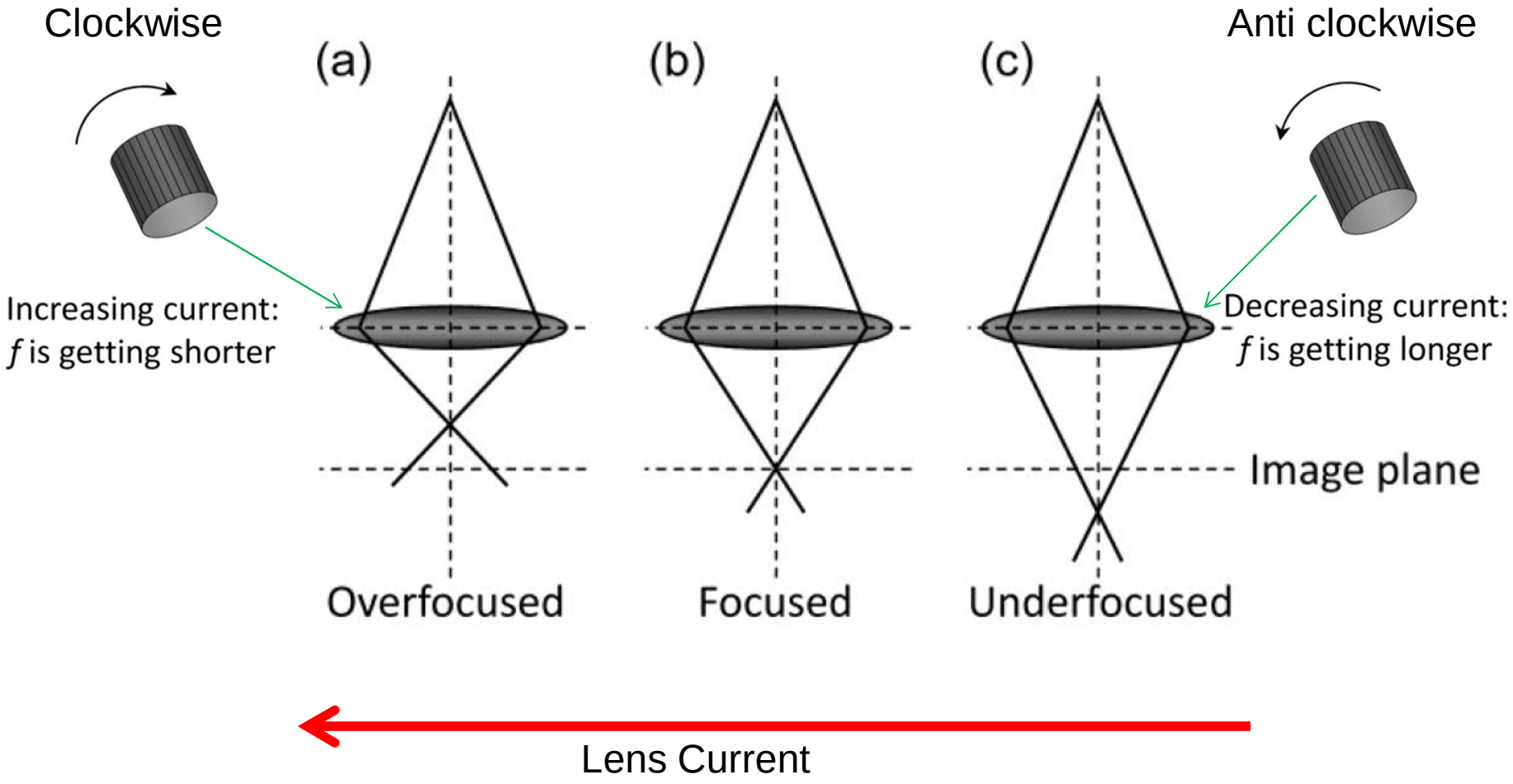

Condenser lenses

C1 => beam size = spot size
C2 => beam intensity = brightness

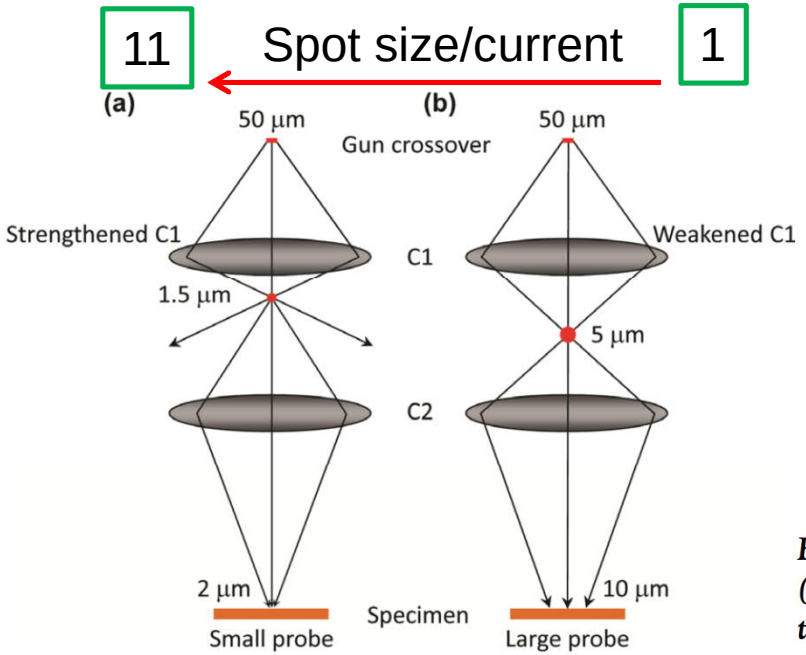

Fig. 3.8 Condenser lens 1 (C1) that controls the beam size. (a) Strengthened C1 to get a small probe on the specimen; (b) weakened C1 to get a large probe on the specimen.

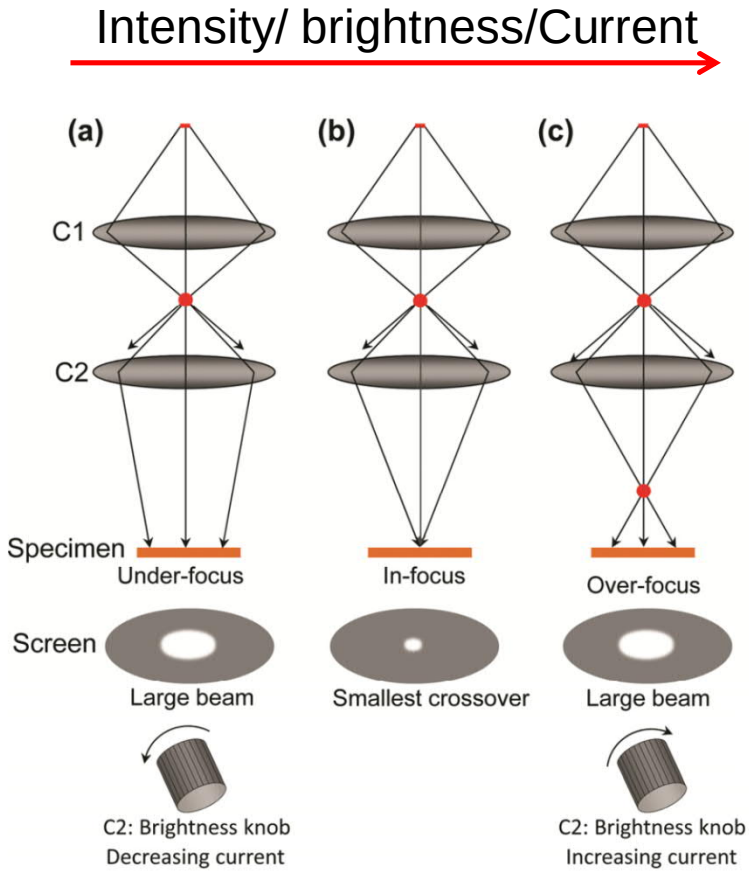

Fig. 3.9 Condenser lens 2 (C2) that controls the beam brightness. (a) Underfocus the beam to get a larger area illumination; (b) in-focus the image to get the smallest beam crossover on the specimen; (c) overfocus the beam to get a larger area illumination. The brightness knob controls C2.

Image mode: C2 lens overfocused!

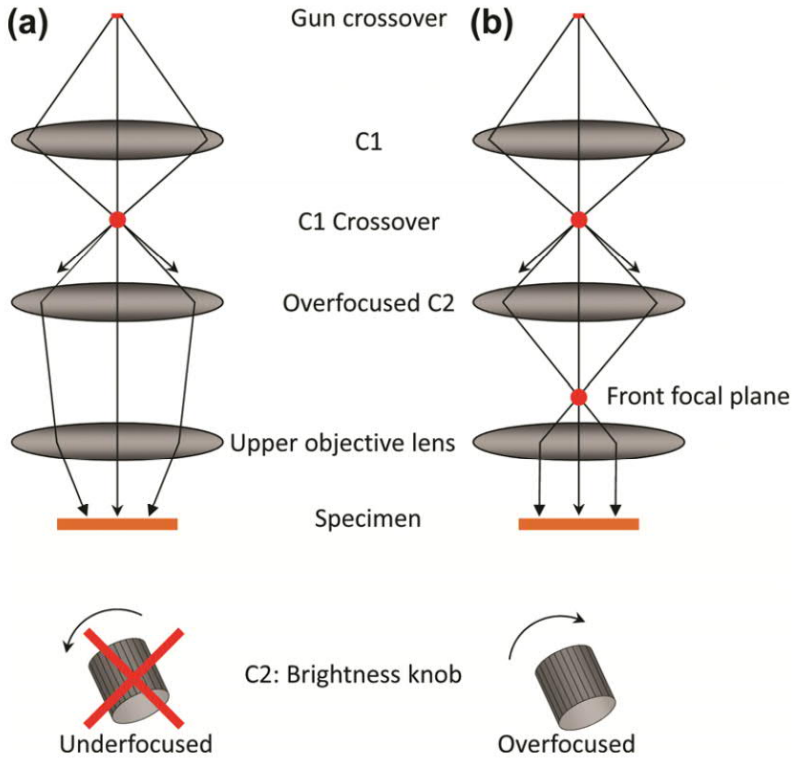

Fig. 3.10 (a) Underfocusing C2 (turning the brightness knob CCW beyond the crossover) results in nonparallel illumination on specimen; (b) overfocusing C2 produces parallel illumination.

Condenser aperture

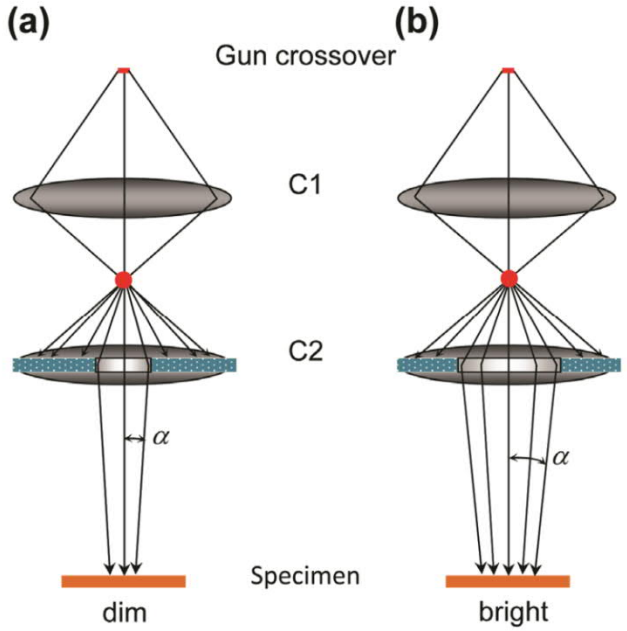

Fig. 3.11 Condenser aperture. (a) Smaller aperture; (b) larger aperture.

Center C2 aperture

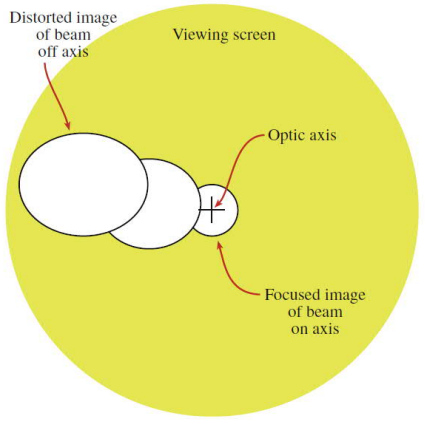

FIGURE 9.7. If the C2 aperture is misaligned, wobbling (alternately underfocusing and overfocusing the C2 lens) causes the image of the beam to sweep off axis (i.e., move across the viewing screen) and to become distorted.

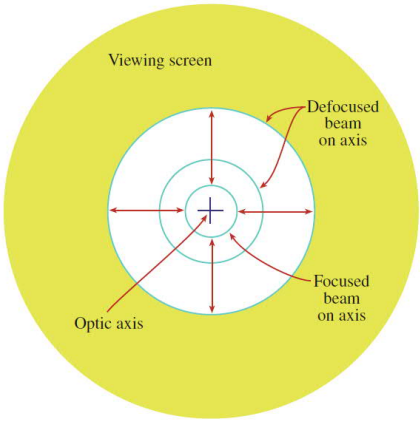

FIGURE 9.8. If the C2 aperture is aligned on axis, the image of the beam remains circular and expands or contracts about the optic axis as C2 is wobbled.

C1: normally fixed, not allowed to change
C2: HRTEM and STEM, smaller, normal TEM 2# or 3#, always center it after change.

Specimen Stage

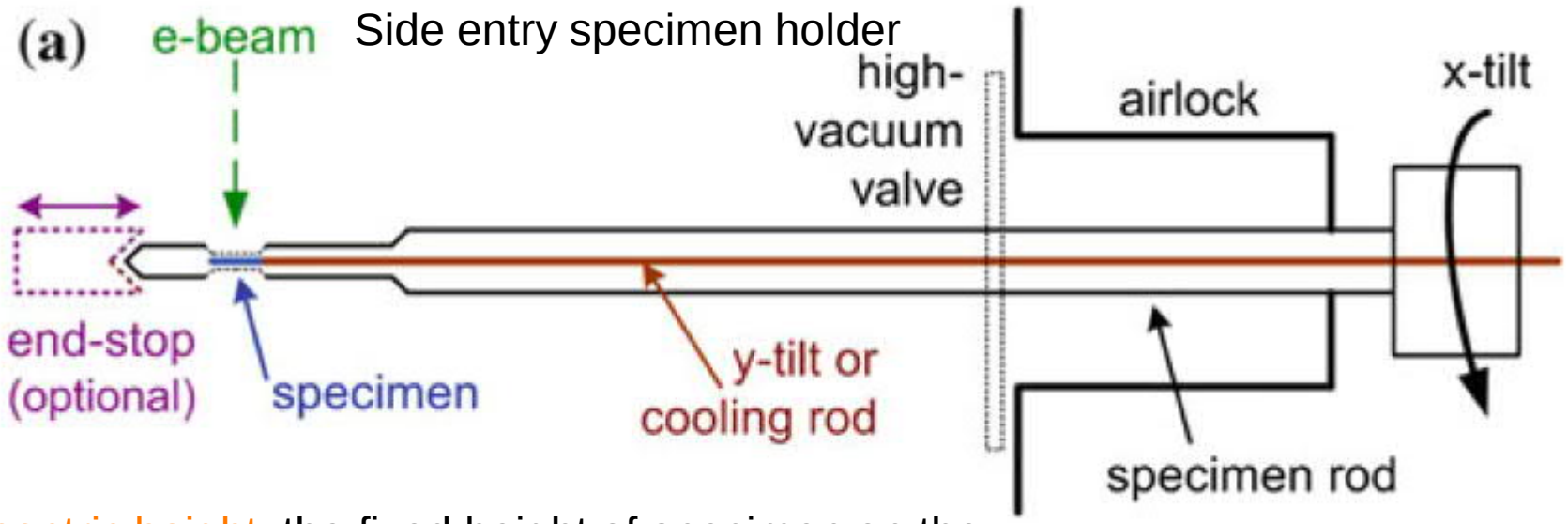

Eucentric height: the fixed height of specimen on the optic axis so we can always work at the **same objective-lens current** and is located also close to the tilt axis of the specimen rod, thus when tilt sample it remains focused.

The central requirement here is the need to define a reference plane so that our calibrations will be reproducible. This plane is eucentric plane.

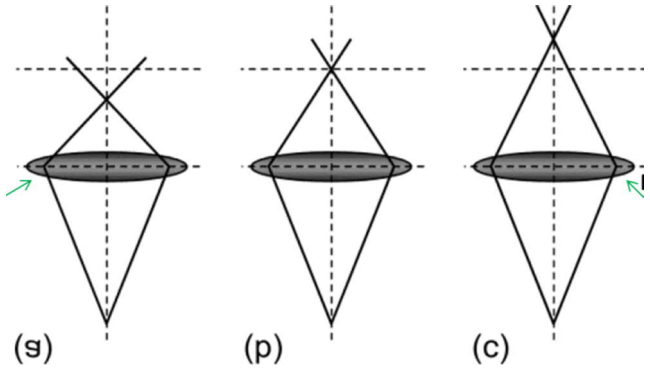

Image system - *Objective lens* and aperture

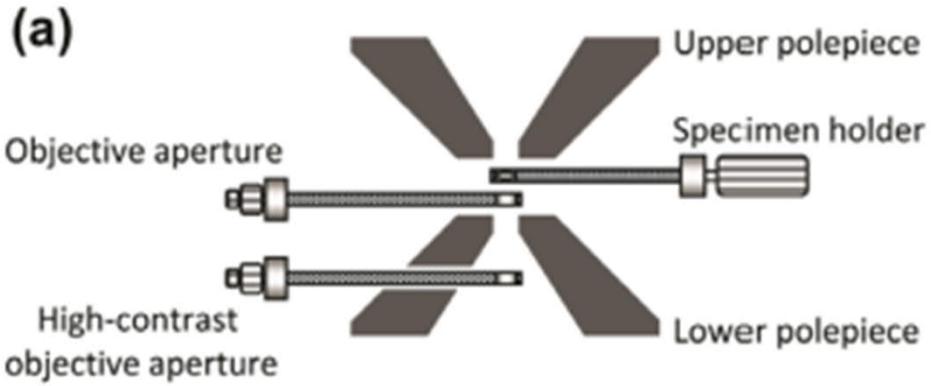

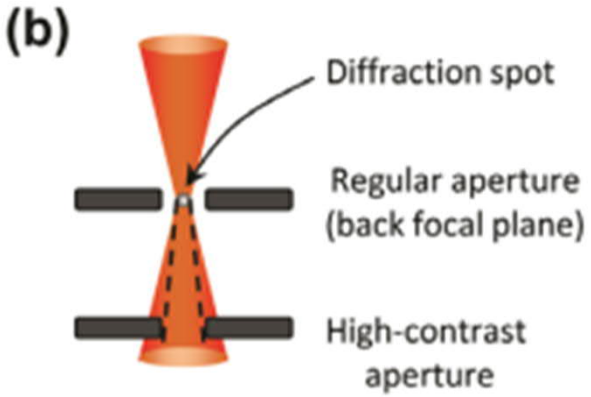

After the electrons pass through the specimen a diffraction pattern is formed in the back focal plane and then the first image is formed at image plane.

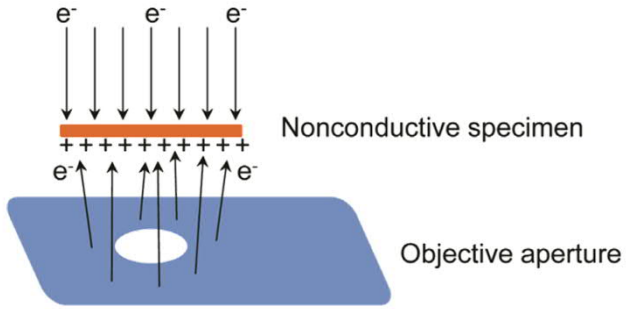

Fig. 3.13 Stabilization of sample by objective aperture under the specimen.

Image system

$$M = M_{\text{Obj}} \times M_{\text{Int}} \times M_{\text{Proj}}$$

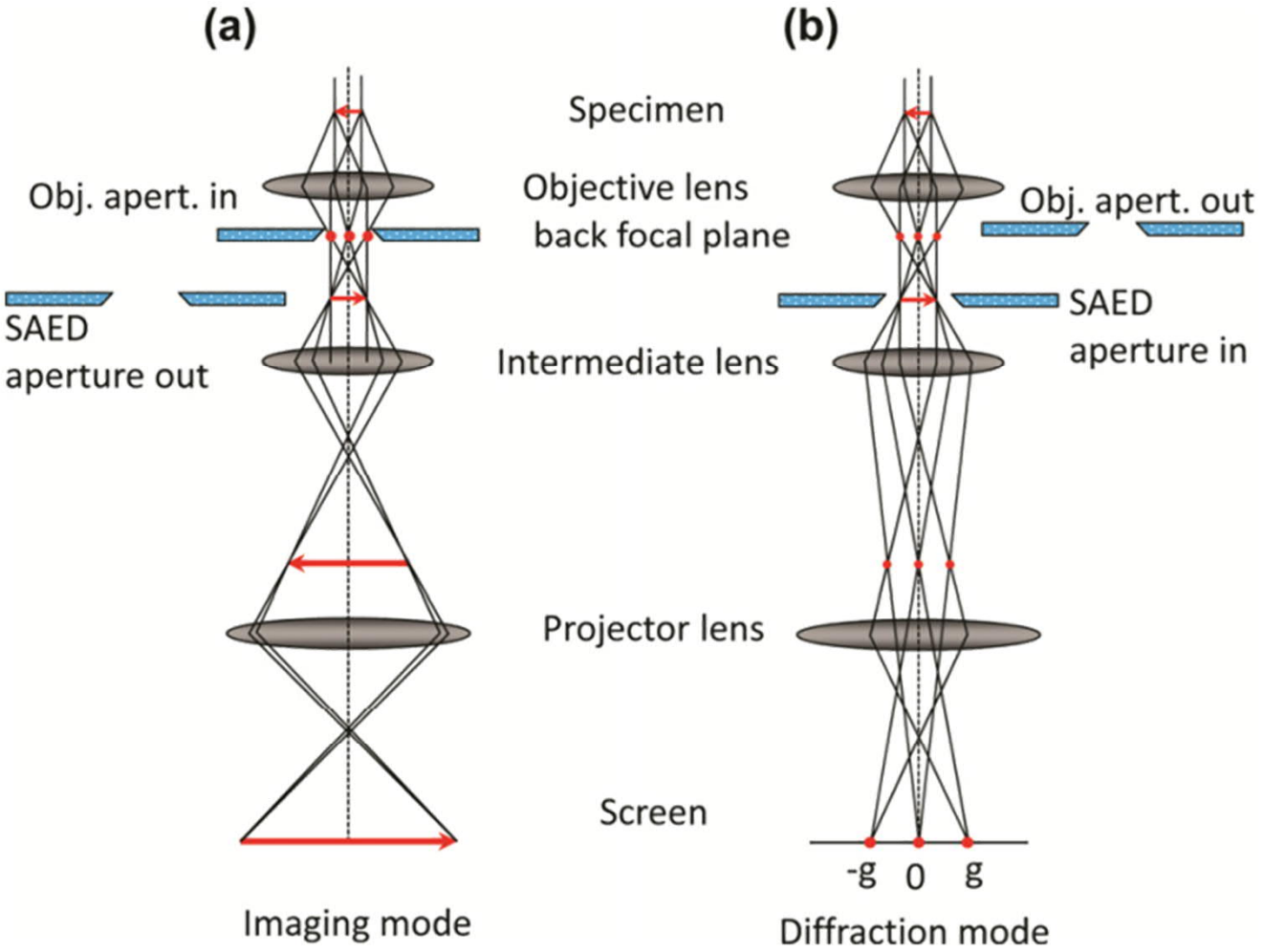

Fig. 3.14 Imaging and diffraction mode determined by intermediate lens. (a) Imaging mode; (b) diffraction mode.

Instrument Imperfections, Alignments, Corrections, and Calibrations

- Spherical Aberration
- Chromatic Aberration
- Astigmatism
- Beam Shift and Beam Tilt
- Depth of Field and Depth of Focus
- Eucentric height - Specimen Height
- Aperture Alignment
- Magnification Calibration
- Camera Length Calibration
- Magnetic Rotation Calibration

TEM instrument is not perfect, imperfections always exist in TEM system. Some of the imperfections can be aligned or corrected at the user level, while some of them have to be done by new designs of the components by manufactures!

Beam Shift and Beam Tilt

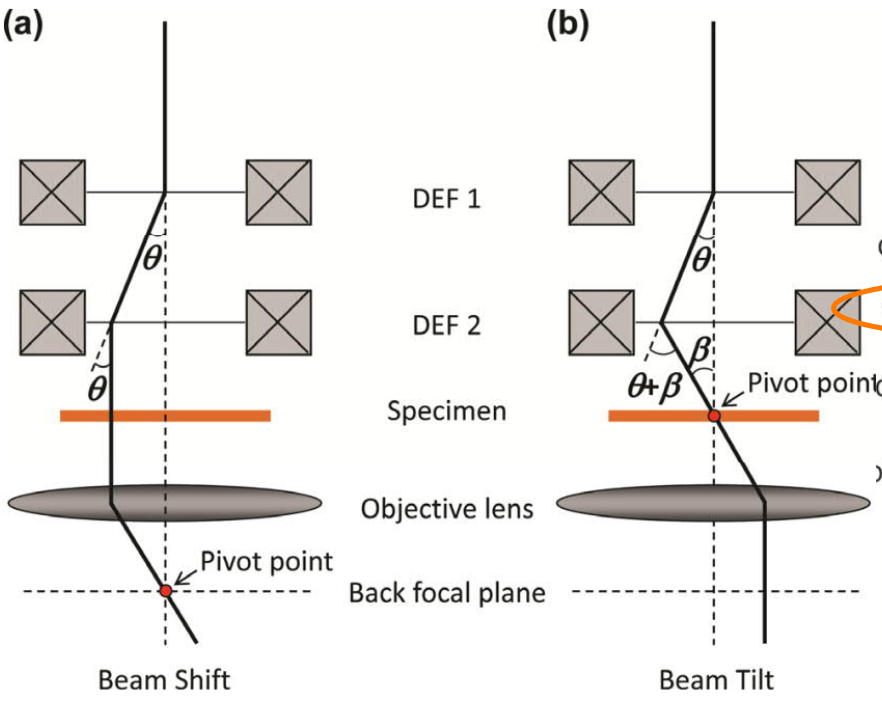

Fig. 3.16 Beam shift (a) and beam tilt (b) by deflector coils.

HRTEM needs to have pure beam shift and beam tilt, then the pivot point need to be centered first.

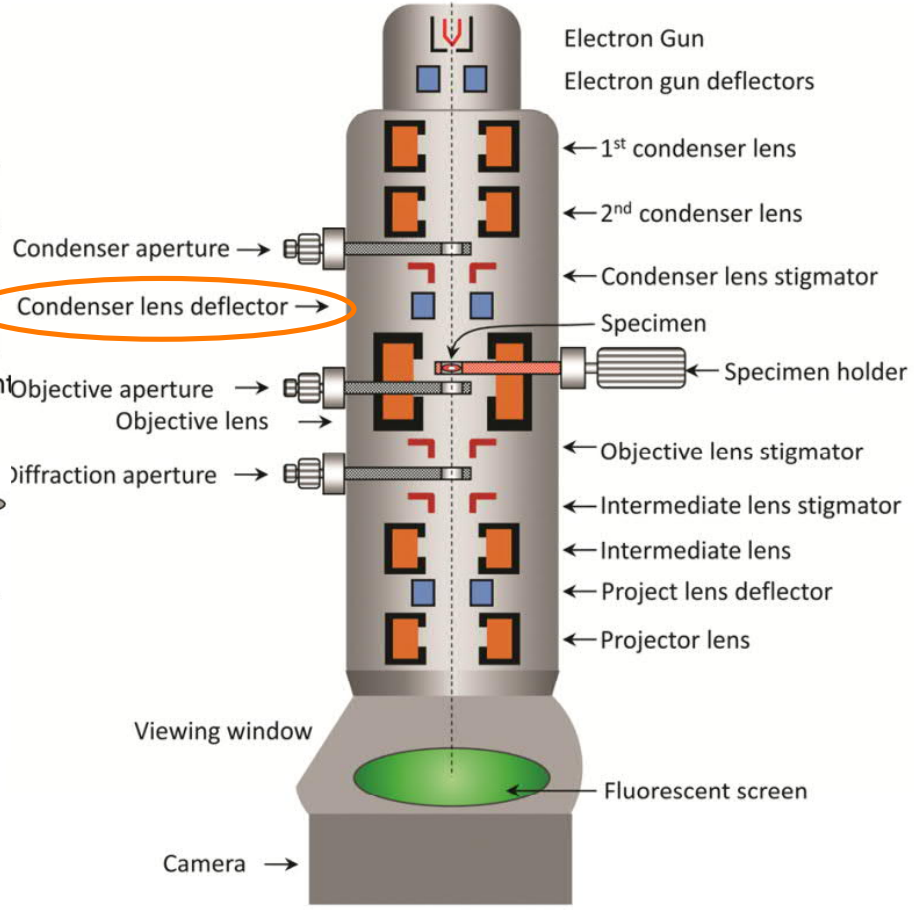

Fig. 3.1 Schematic construction of a TEM.

Spherical Aberration

$$r_{sph} = C_S \beta^3$$

Cs approximately equal to the focal length of the lens, which for **objective lenses** in most TEMs is 1-3mm but in high-resolution instruments may be well below 1 mm if you have a Cs **corrector.**

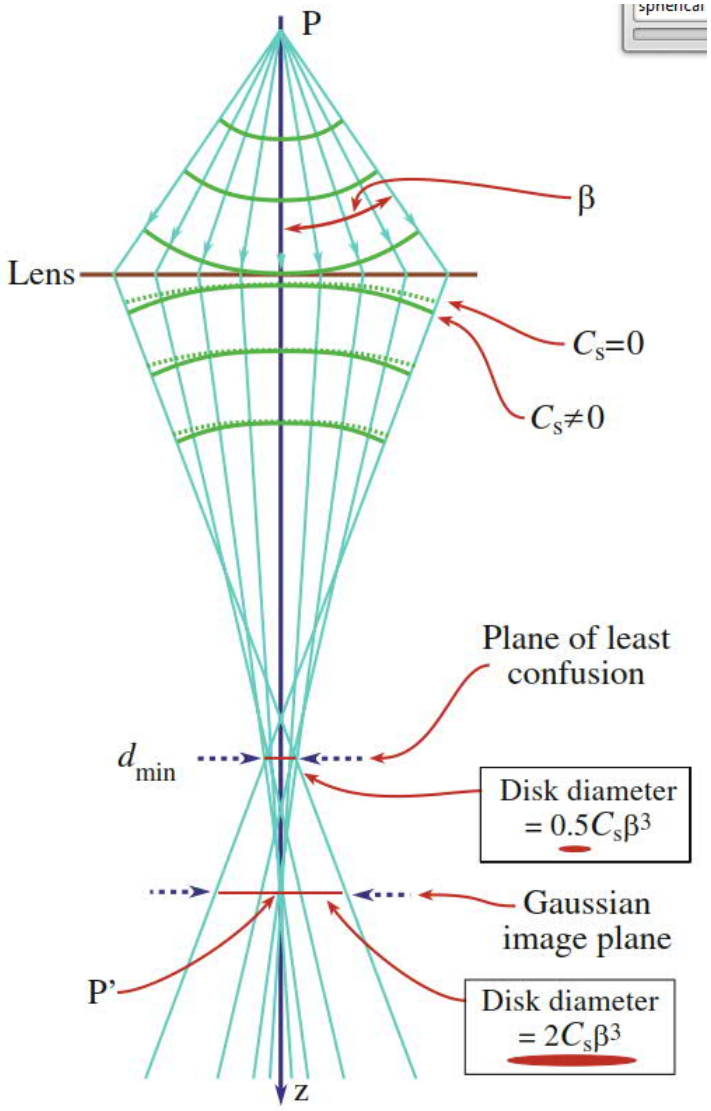

FIGURE 6.11. Spherical aberration in the lens causes wavefronts from a point object P to be spherically distorted by bending the rays at the outside of the lens more than those close to the axis. The point is thus imaged as a disk with a minimum radius in the plane of least confusion and a larger disk at P′ in the Gaussian-image plane. The plane of least confusion is where the smallest image of the object is formed. Schematic intensity distributions at these two important planes are shown beside the ray diagram.

Chromatic Aberration

$$r_{chr} = C_C(\Delta E/E_0)\beta$$

Cc like Cs, is a length, approximately equal to the focal length.

Solution:

- monochromator, which is very expensive;
- thin sample;
- energy filter TEM (EFTEM)

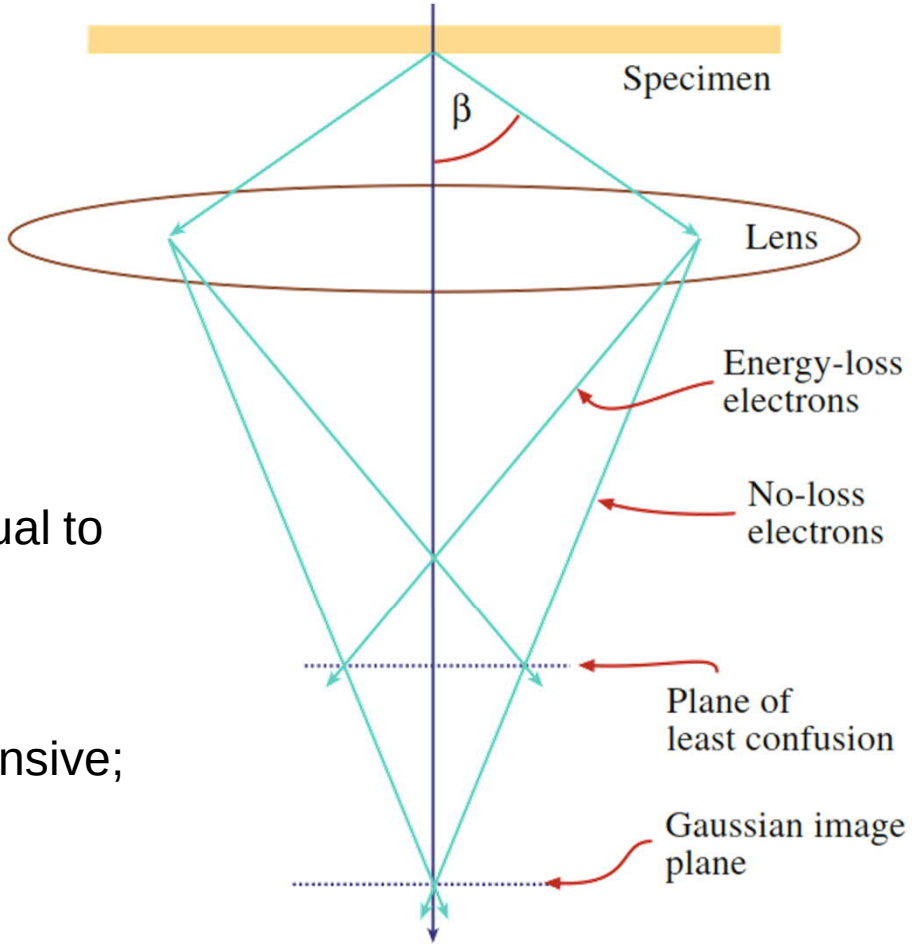

FIGURE 6.13. Chromatic aberration results in electrons with a range of energies being focused in different planes. Electrons emerging from the specimen with no loss of energy are less strongly focused than those that suffered energy loss within the specimen. So, as in Figure 6.11, a point in the object is imaged as a disk in the Gaussian image plane and there is a plane of least confusion.

Astigmatism

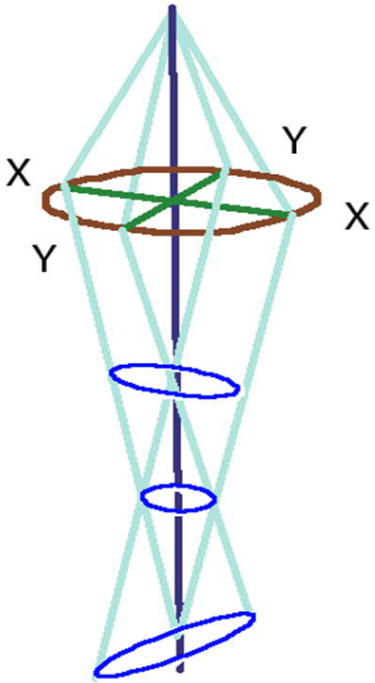

Correct condense astigmatism

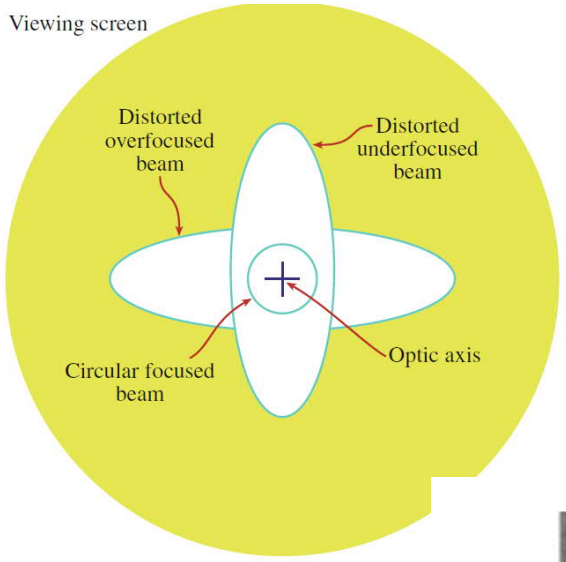

FIGURE 9.9. The effect of astigmatism in the illumina distort the image of the beam elliptically as the C2 Correction of this astigmatism results in an image that as the C2 lens is defocused (as in Figure 9.8).

$$r_{ast} = \beta \Delta f$$

Astigmatism is caused by asymmetrical field can be corrected by stigmators.

Fresnel Fringes

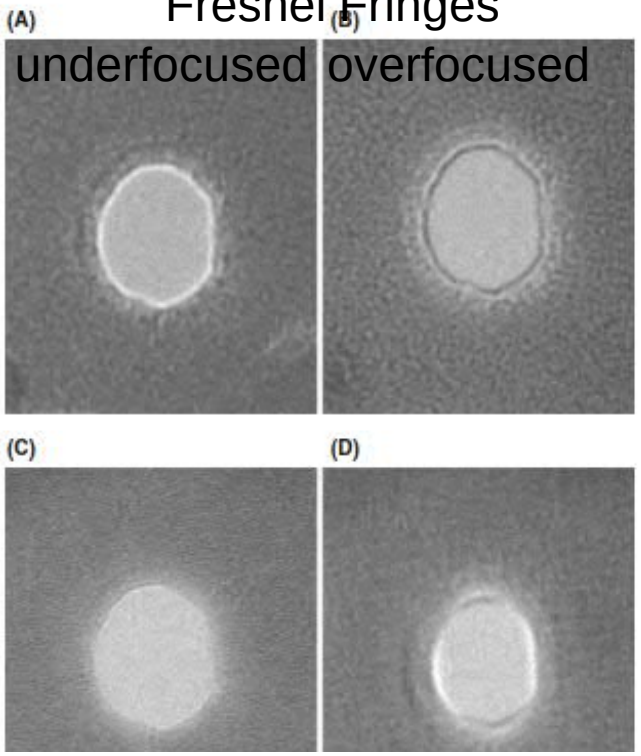

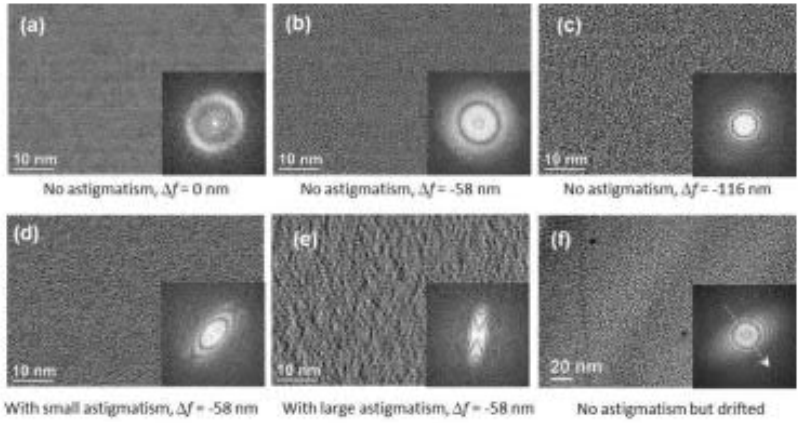

Fig. 3.22 Correction of objective lens astigmatism using FFT. (a–c) No astigmatism but at different defocus Δf; (d, e) with astigmatism at different defocus Δf; (f) no astigmatism but the sample drifts along the direction indicated with an arrow.

Depth of focus and depth of field

The depth of field, D_{ob}, is measured at, and refers to, the *object plane*. It's the distance along the axis on both sides of the object plane within which we can move the object without loss of focus in the image.

$$D_{ob} = \frac{d_{ob}}{\beta}$$

The depth of focus, D_{im}, is measured in, and refer to, the *image plane*. It is the distance along the axis on both sides of the image plane within which the image appears focused (assuming the object plane and objective lens are fixed.)

$$M = \frac{d_{im}}{d_{ob}} = \frac{\beta}{\alpha} \qquad D_{im} = \frac{d_{im}}{\alpha} = \frac{d_{ob}}{\beta} M^2$$

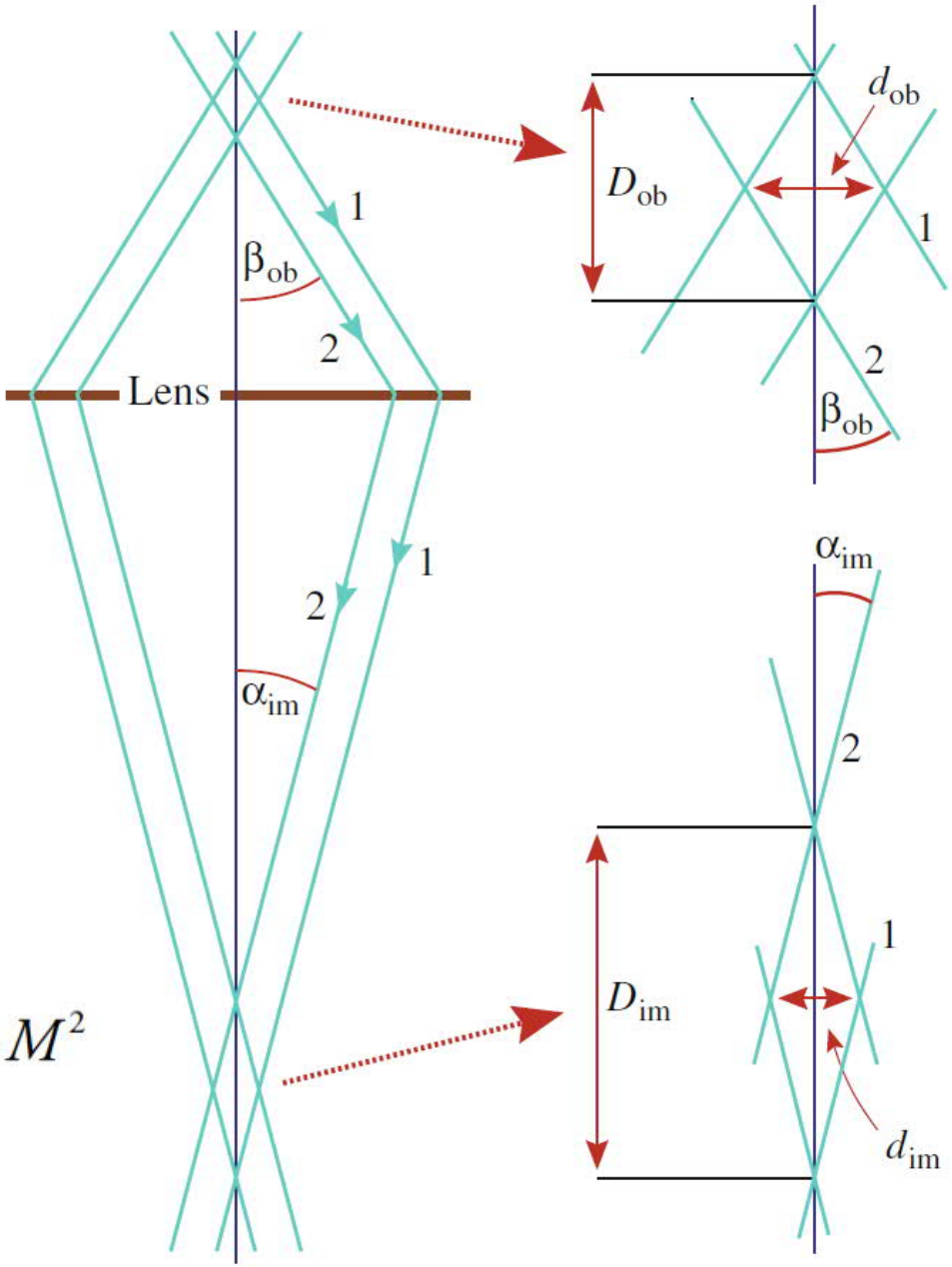

Eucentric height – specimen height

- The eucentric position is the horizontal center of the objective lens.
- TEMs are set up so that **magnification**, **camera length**, and **correct focus** are set to this reference position. When the sample height (in the Z-direction) is set at the eucentric position, one can tilt the sample around its axis without the image of the sample moving across the projection screen.
- The sample must be set to this position. To do this first adjusting the objective lens current to a specific known setting for a specific voltage and then the entire sample holder is raised or lowered.

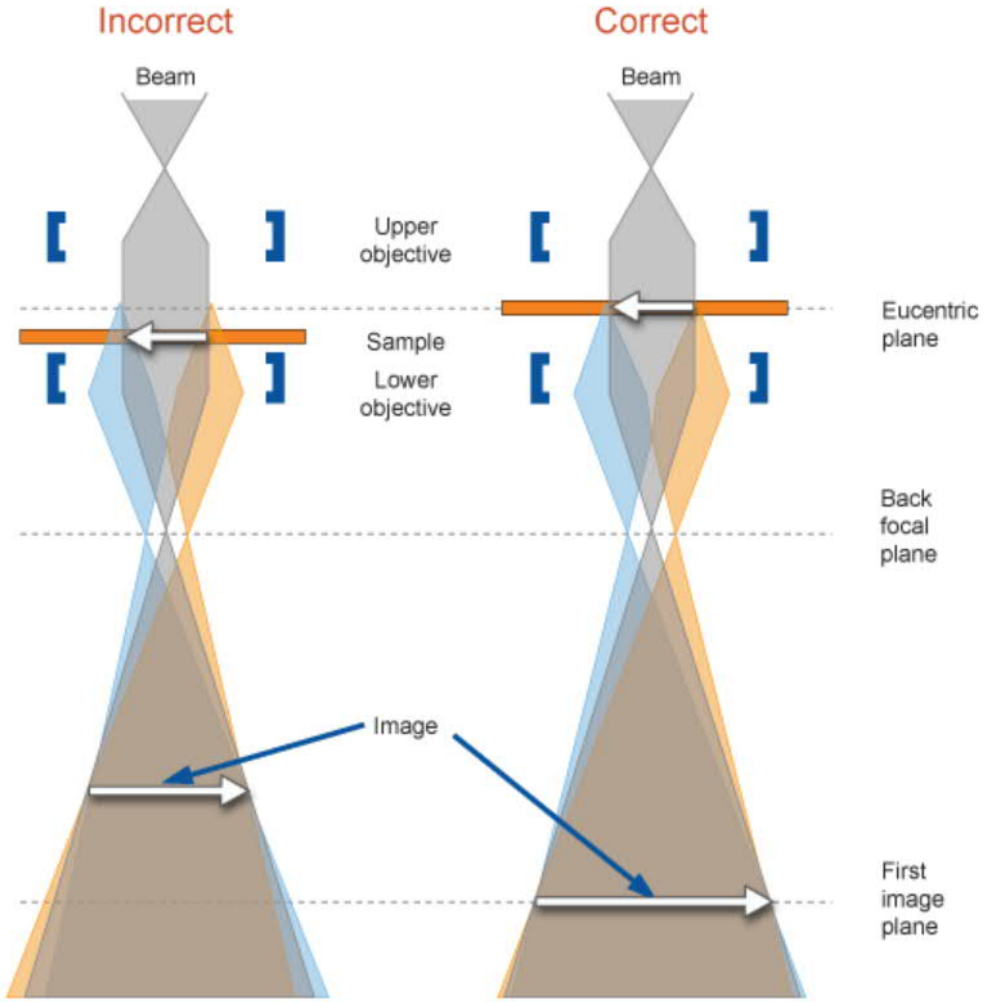

http://www.ammrf.org.au/myscope/tem/background/concepts/imagegeneration/diffraction/eucentric/

Camera-Length Calibration

The magnification of the DP is described by the camera length (L). The camera length is a calculated value rather than a physical distance.

$$2\theta = r/L,$$
$$2\sin\theta = \lambda/d.$$

$$rd = \lambda L$$

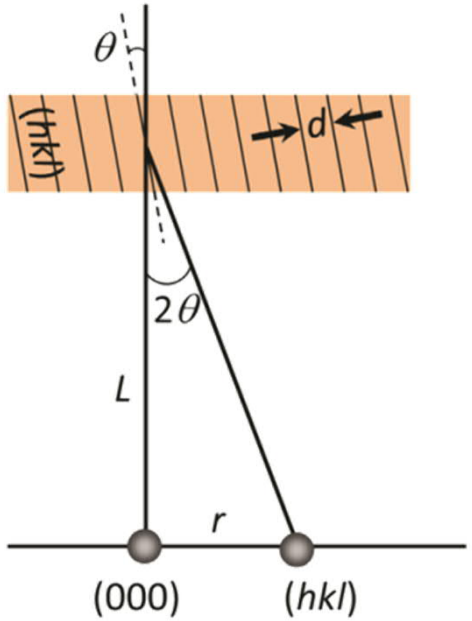

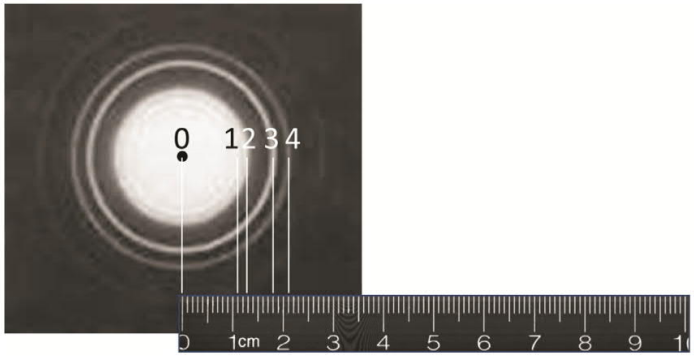

Fig. 3.26 Camera length calibration using polycrystalline Al thi and the SAED pattern is taken on a film.

Table 3.4 Example of CL calibration showing the nominal and calibrated CL.

Nominal CL (cm)	Calibrated CL (cm)	Error (%)	Camera constant (Å·mm)
150	152.99	1.99	38.4
100	102.39	2.39	25.7
80	79.8	–0.25	20.03
60	59.63	–0.62	14.97
50	51.2	2.40	12.85
40	40.91	2.27	10.27

Microscopy and the Concept of Resolution

Rayleigh criterion for visible light microscopy

$$\delta = \frac{0.61\lambda}{\mu \sin \beta}$$

δ: point resolution

λ: wavelength

μ: refractive index

β: semi-angle of the lens

$\mu \sin\beta \approx 1, \delta \approx 0.61\lambda$

For TEM the approximate:

$$\delta \approx 1.22\lambda/\beta$$

TABLE 1.2 Electron Properties as a Function of Accelerating Voltage

Accelerating voltage (kV)	Non-relativistic wavelength (nm)	Relativistic wavelength (nm)	Mass ($\times m_0$)	Velocity ($\times 10^8$ m/s)
100	0.00386	0.00370	1.196	1.644
120	0.00352	0.00335	1.235	1.759
200	0.00273	0.00251	1.391	2.086
300	0.00223	0.00197	1.587	2.330
400	0.00193	0.00164	1.783	2.484
1000	0.00122	0.00087	2.957	2.823

The resolution of the electron lens and TEM

Definition: resolution is defined as the minimum-resolvable distance in the object to be distinguished by the microscope.

1. Theoretical resolution (diffraction limited resolution).
   $r_{th} = 1{,}22\lambda/\beta$
2. The practical resolution due to **spherical aberration**.
   $r_{min} \approx 0{,}91(C_S\lambda^3)^{1/4}$.
3. Specimen-limited resolution duo to **chromatic aberration**.
   $r_{chr} = C_C(\Delta E/E_0)\beta$, $r_{chr} \sim$ 2.5nm, for ΔE=25eV, E=100keV, β=4.5mrad. This is resolution limit in most of case! **Thinner is better**!
4. Line resolution or lattice fringes

FFT of HRTEM image, normal TEM 0.1Å, Cs corrected can be reach 0.01Å.

Electron Diffraction

Interaction of Electrons with Matter

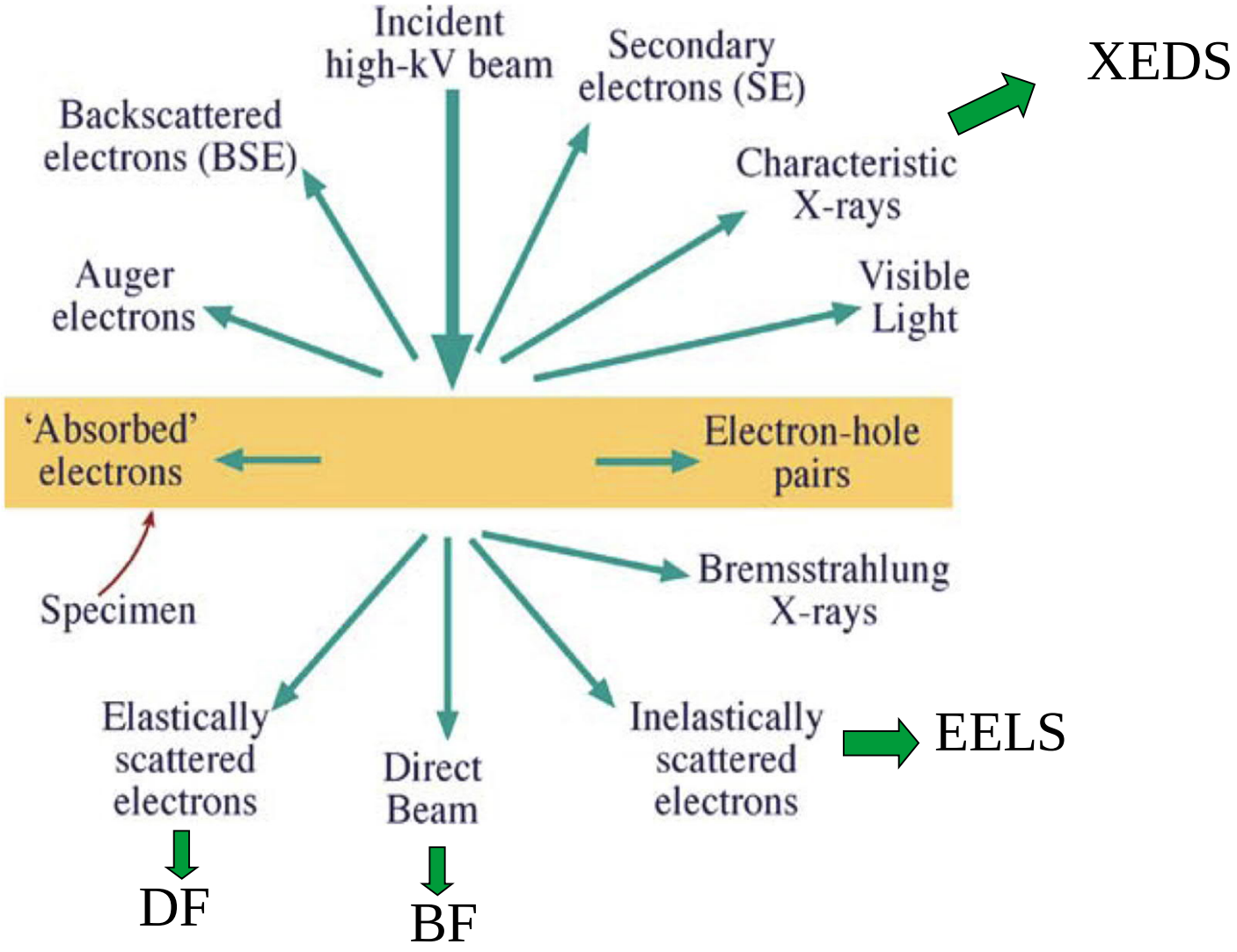

Bragg's law in vector

When θ equals the Bragg angle, θ_B:

AC+CD = $2d\sin\theta_B = n\lambda$

$$2\sin\theta_B = \frac{\lambda}{d} \qquad |\mathbf{K}| = \frac{2\sin\theta_B}{\lambda}$$

$|\mathbf{K}_B| = 1/d, \quad \mathbf{K}_B = \mathbf{g}$

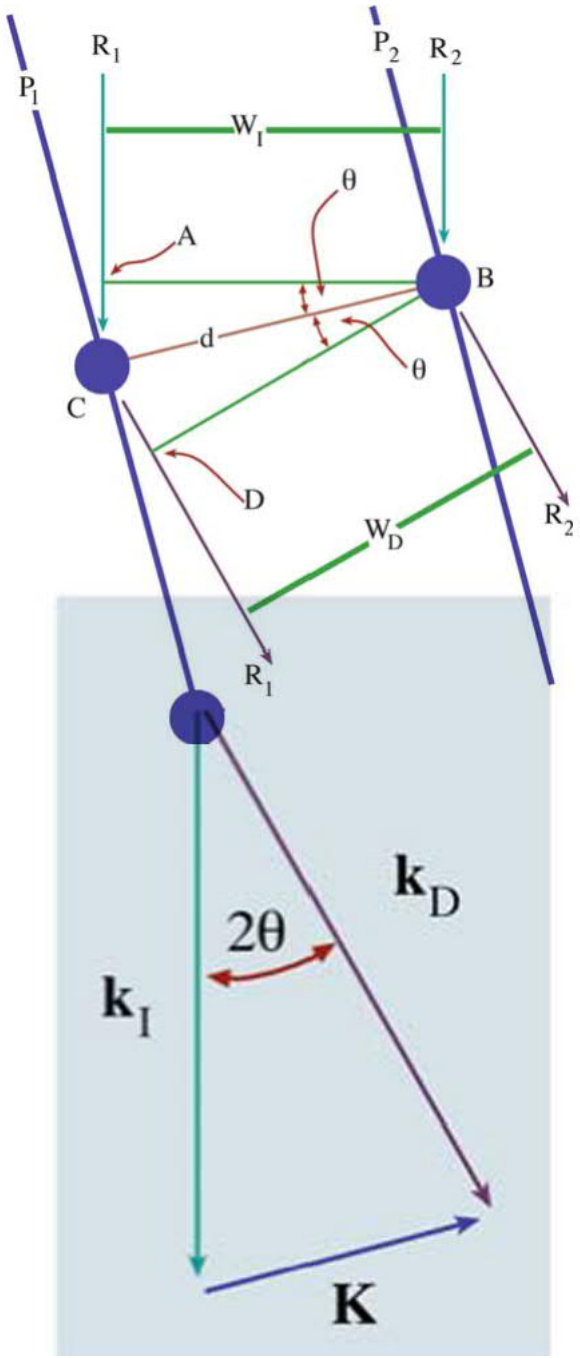

The vector g

The definition of the (*hkl*) indices is OA = *a*/*h*; OB = *b*/*k*: OC = *c*/*l*. the plane ABC can then be represented as (*hkl*).

$$\mathbf{g}_{hkl}^{*} = h\mathbf{a}^{*} + k\mathbf{b}^{*} + l\mathbf{c}^{*}$$

$$|\mathbf{g}| = 1/d_{hkl}$$

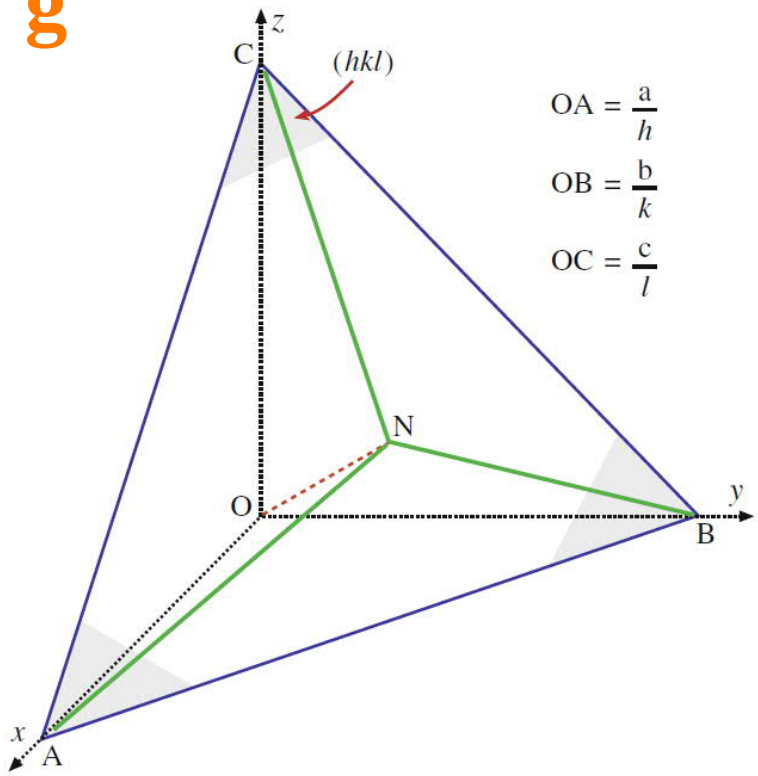

Vector $\mathbf{g}_{hkl}$ is normal to the plane (*hkl*) and its length is ($1/d_{hkl}$).

TABLE 12.1. Notation for Planes, Directions, and Reflections

Real space	Reciprocal space	
Particular direction	Particular plane	[*UVW*]
General direction	General plane	<*UVW*>
Particular plane	Particular direction	(*hkl*)
General plane	General direction	{*hkl*}
Diffracting plane	Indexed reflection	*hkl*

The Ewald Sphere of Reflection

Construction of Ewald sphere, start from the origin O of reciprocal-lattice and from O to have incident vector length 1/λ as a radius to get the center of Ewald sphere C.

The key point is that when the sphere cuts through the reciprocal-lattice point the Bragg condition is satisfied.

$\mathbf{k}_D$ could be any vector which begins at C and ends on the sphere.

The origin O of reciprocal-lattice is fixed, not the center of sphere C, which moves with incident beam.

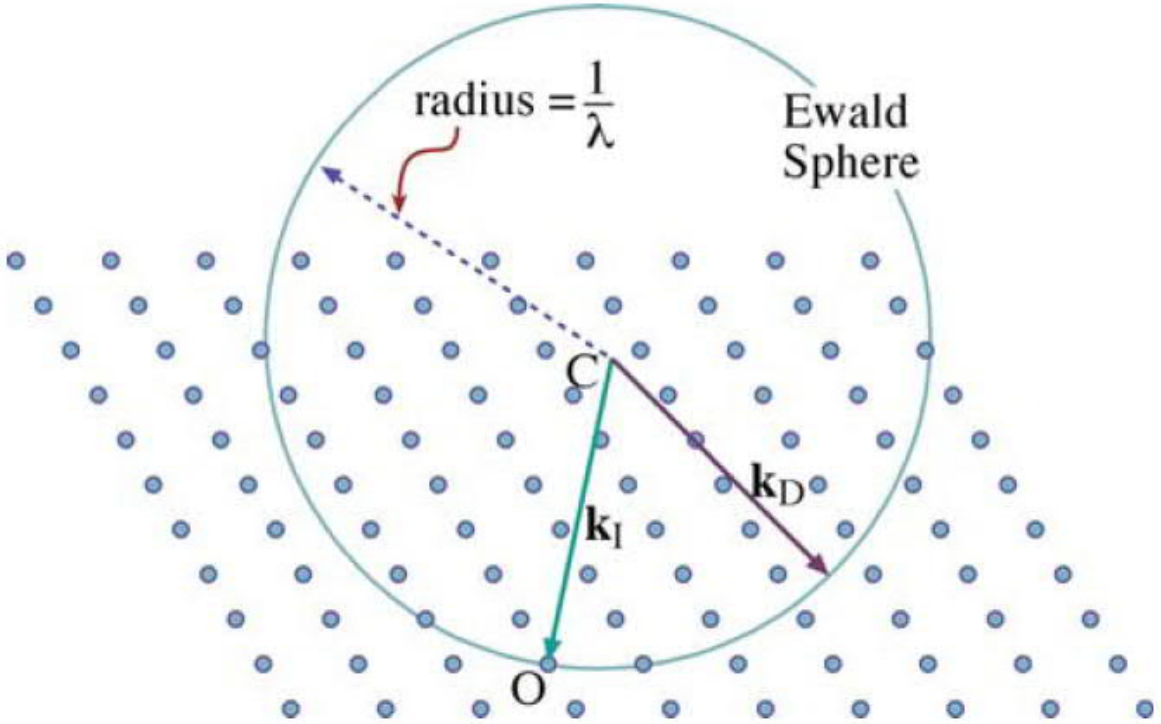

FIGURE 12.3. The Ewald sphere of reflection is shown intersecting a non-cubic array of reciprocal-lattice points. The vector **CO** represents $\mathbf{k}_I$, the wave vector of the incident wave, and O is the origin of the reciprocal lattice. $\mathbf{k}_D$ is any radius vector. When the radius of the sphere is similar to the spacing between the points in the reciprocal lattice, as is the case for X-rays, the sphere can only intersect a few points. When λ is much smaller, as for 100-keV electrons, the radius is much larger, the sphere is flatter, and it intersects many more points.

Selected-Area Diffraction

- Determination of crystal structure
- Phase identification, crystallographic orientations
- Align the specimen orientation for imaging.

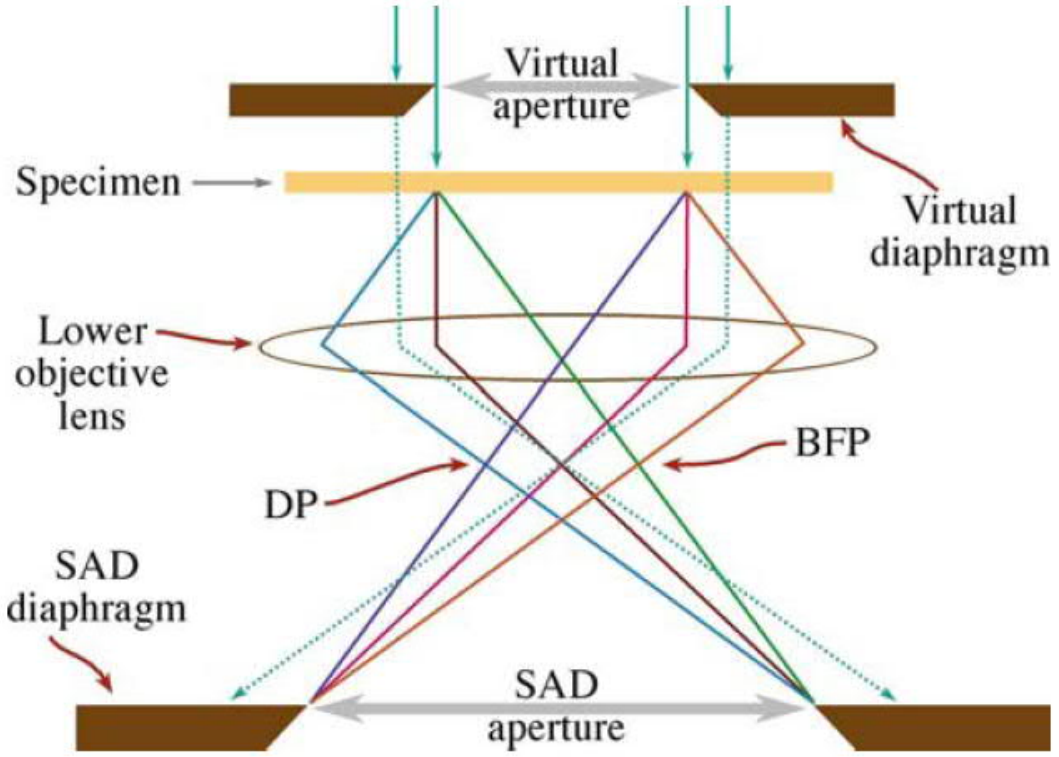

FIGURE 9.13. Ray diagram showing SADP formation: the insertion of an aperture in the image plane results in the creation of a virtual aperture in the plane of the specimen (shown here slightly above the specimen plane). Only electrons falling inside the dimensions of the virtual aperture at the entrance surface of the specimen will be allowed through into the imaging system to contribute to the SAD pattern. All other electrons (dotted lines) will hit the SAD diaphragm.

Indexing of Powder Patterns

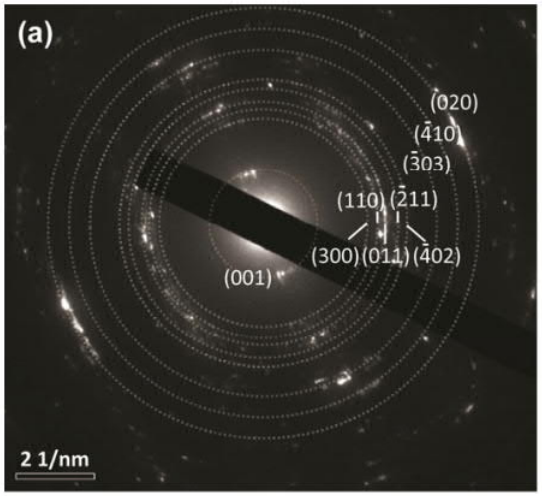

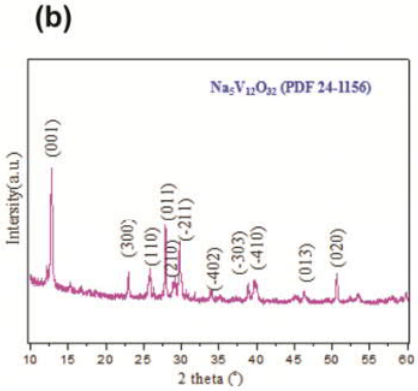

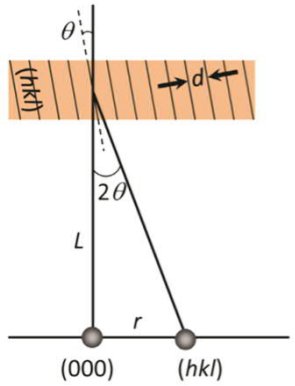

$$d = \frac{L\lambda}{r}$$

Fig. 4.8 Comparison of SAED and XRD patterns from $Na_5V_{12}O_{32}$. (a) Indexing of a powder SAED pattern; (b) indexing of XRD pattern

Table 4.1 Indexing of diffraction rings of Fig. 4.8(a).

No.	SAED	XRD			*h*	*k*	*l*
	d (Å)	*d* (Å)	Theta	Intensity			
1	7.11	7.01	6.309	100	0	0	1
2	3.90	3.87	11.481	50	3	0	0
3	3.47	3.45	12.901	70	1	1	0
4	3.23	3.22	13.84	90	0	1	1
5	2.94	2.988	14.939	50	–2	1	1
6	2.76	2.64	16.964	30	–4	0	2
7	2.29	2.318	19.409	50	–3	0	3
8	2.12	2.269	19.845	30	–4	1	0
9	1.83	1.807	25.231	80	0	2	0

Single Crystal Diffraction Patterns

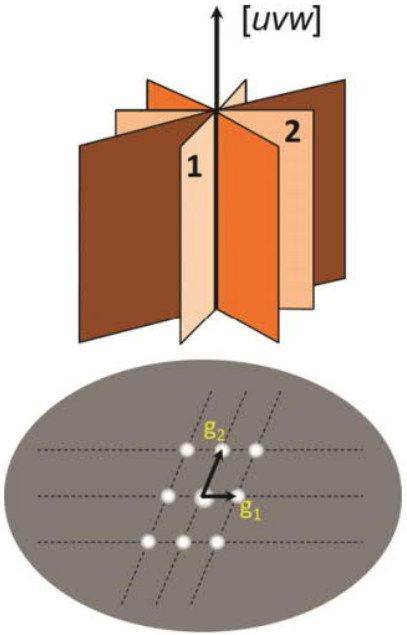

Weiss Zone law

$$\mathbf{g}_{hkl} \cdot [UVW] = 0$$

$$hU + kV + lW = 0$$

Accordingly, if any two vectors that are not in a line are known, the zone axis can be obtained by

$$[UVW] = \mathbf{g}_1 \times \mathbf{g}_2 = \begin{vmatrix} i & j & k \\ h_1 & k_1 & l_1 \\ h_2 & k_2 & l_2 \end{vmatrix} = \begin{vmatrix} k_1 & l_1 \\ k_2 & l_2 \end{vmatrix} i - \begin{vmatrix} h_1 & l_1 \\ h_2 & l_2 \end{vmatrix} j + \begin{vmatrix} h_1 & k_1 \\ h_2 & k_2 \end{vmatrix} k$$

$$= (k_1 l_2 - l_1 k_2) i - (h_1 l_2 - l_1 h_2) j + (h_1 k_2 - k_1 h_2) k \qquad (4.16)$$

and therefore,

$$U = (k_1 l_2 - l_1 k_2), \quad V = -(h_1 l_2 - l_1 h_2), \quad W = (h_1 k_2 - k_1 h_2) \qquad (4.17)$$

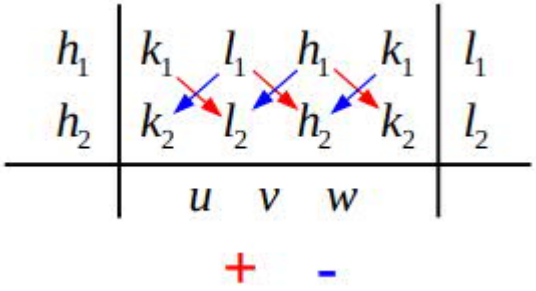

Indexing of Single Crystal Diffraction Patterns

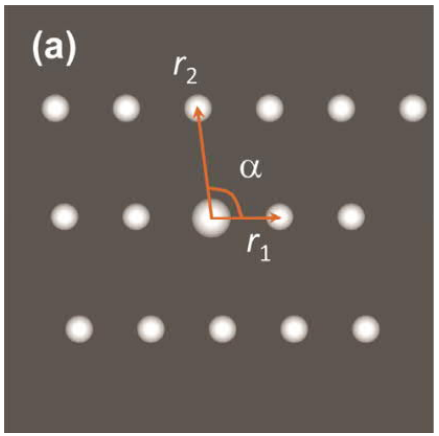

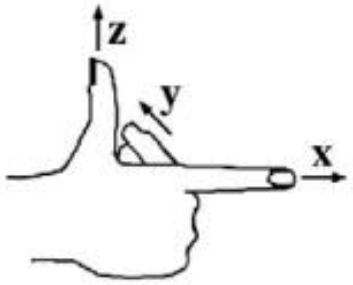

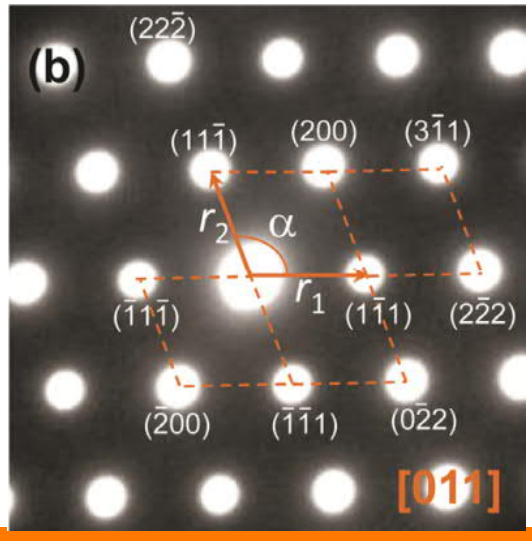

FCC ZA [011]

1. Measure lengths of two independent shortest reciprocal vectors r_1 (the shortest one) and r_2 (the shortest if available, or the second shortest one) and angle between them α.
2. Calculate the ratio of r_2/r_1 (>=1) and the greatest lattice spacing d1 using $d_1=(L\lambda)/r_1$, or using CCD acquisition software with a calibration.
3. If the structure is known, computer all possible zone axis patterns in order of the ratio of r_2/r_1 and angle α, and then find out the indexes of $(h_1k_1l_1)$ and $(h_2k_2l_1)$.

TEM imaging

- **Scattering contrast or Amplitude Contrast**

  mass-thickness contrast

  diffraction contrast

  Thickness and Bending Effects

  Planer defects

  dislocations

- **Phase Contrast Images**

  high resolution TEM

What is contrast?

$$C = \frac{(I_2 - I_1)}{I_1} = \frac{\Delta I}{I_1}$$

For eyes > 5-10%, 16 gray level

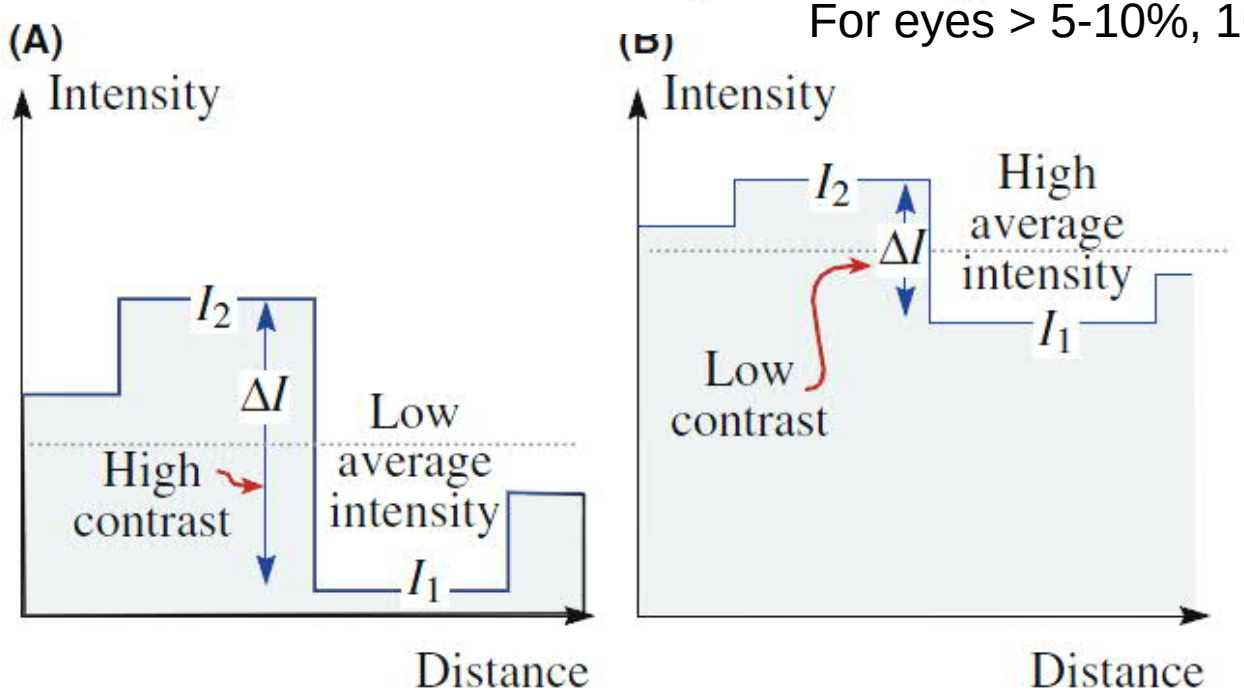

FIGURE 22.1. Schematic intensity profiles across an image showing (A) different intensity levels (I_1 and I_2) and the difference (ΔI) between them which defines the contrast. Generally, in a TEM, if the overall intensity is increased (B) the contrast decreases.

Mass-Thickness Contrast

Scattering angle ↑

High contrast

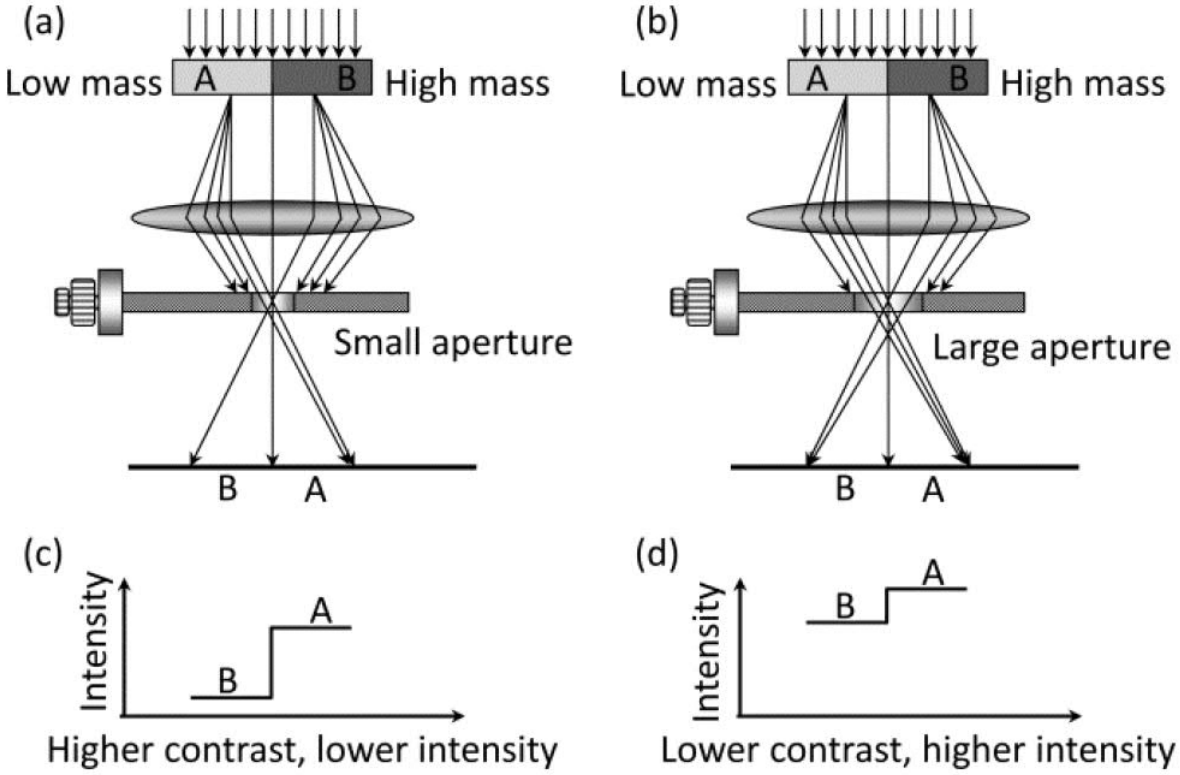

Fig. 5.2 Mass-thickness contrast. Grain A has a low mass and grain B has high mass. A small objective aperture is used in (a) while a large aperture is used in (b), yielding higher contrast (while lower image intensity) and lower contrast (while higher image intensity), as shown in (c) and (d), respectively.

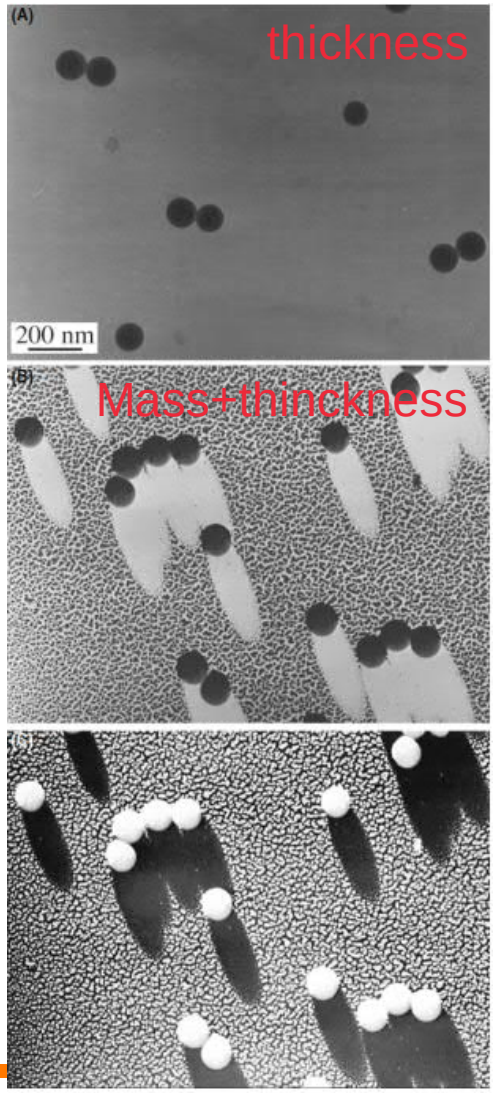

FIGURE 22.5. (A) TEM BF image of latex particles on a carbon support film showing thickness contrast only. (B) Latex particles on a carbon film shadowed to reveal the shape of the particles through the addition of selective mass contrast to the image. (C) Reverse print of (B) exhibits a 3D appearance.

Diffraction Contrast

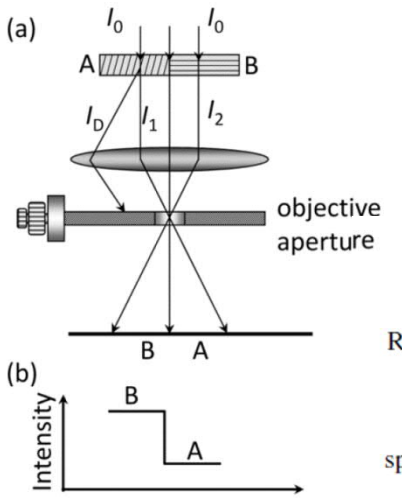

Fig. 5.3 (a) Formation of diffraction contrast; (b) image intensity.

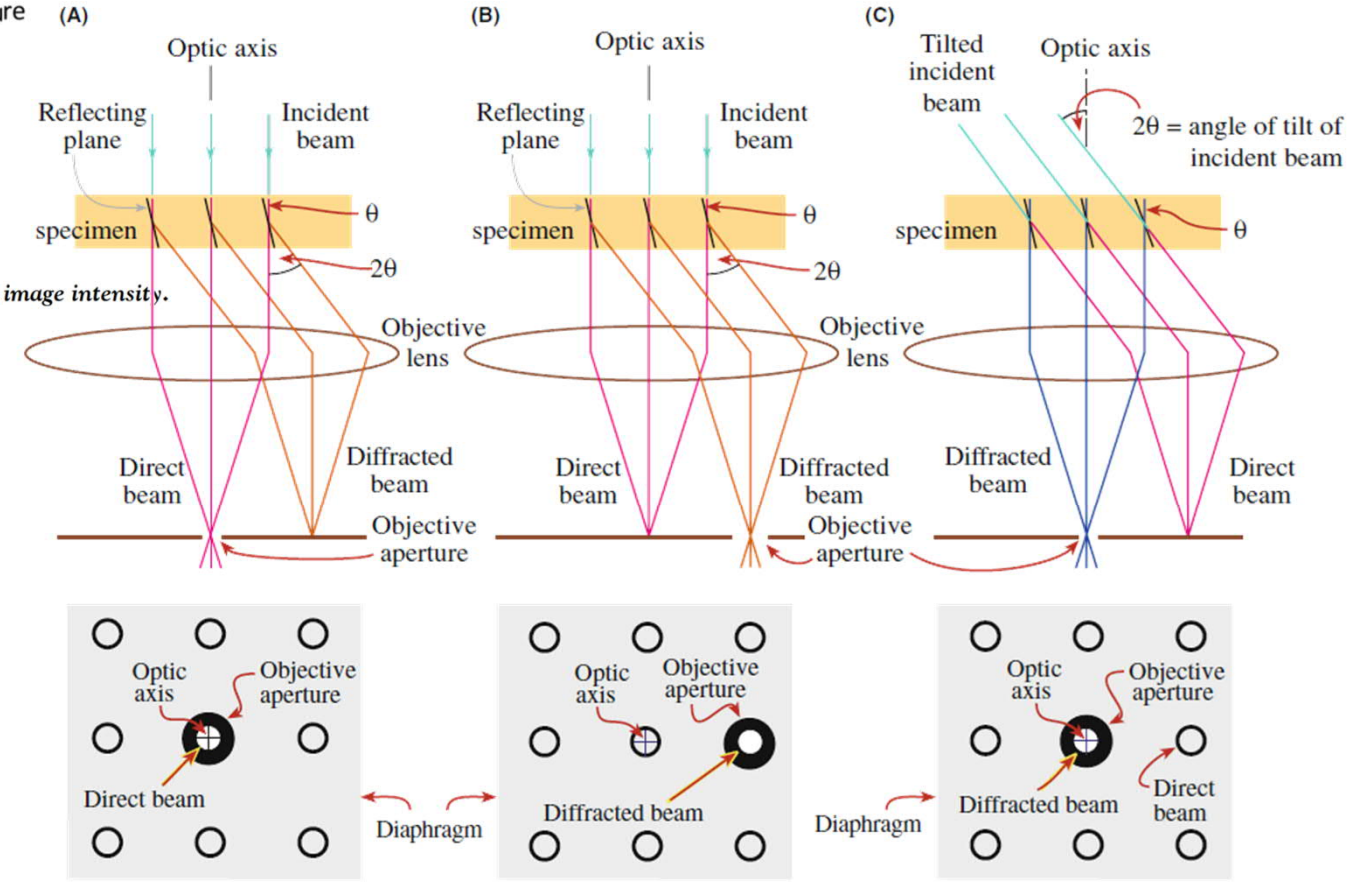

FIGURE 9.14. Ray diagrams showing how the objective lens and objective aperture are used in combination to produce (A) a BF image formed from the direct electron beam, (B) a displaced-aperture DF image formed with a specific off-axis scattered beam, and (C) a CDF image where the incident beam is tilted so that the scattered beam emerges on the optic axis. The area of the DP selected by the objective aperture, as seen on the viewing screen, is shown below each ray diagram. (Images comparing BF and DF are given in Part 3.)

Diffraction Contrast - example

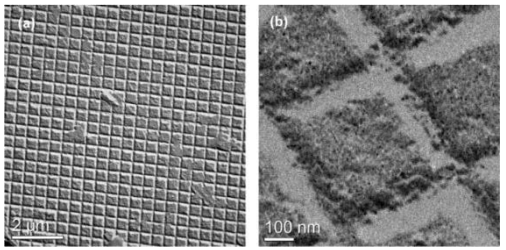

Diffraction mode

Image mode

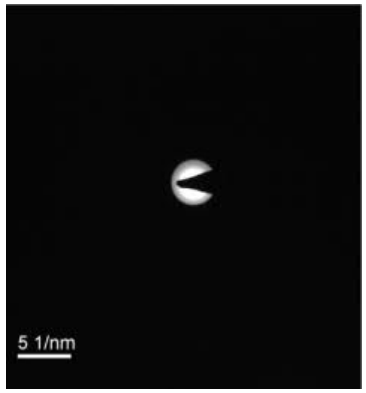

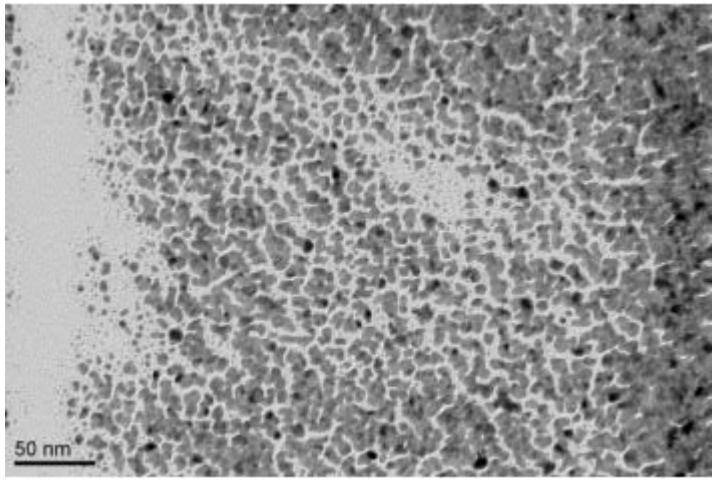

Bright Field

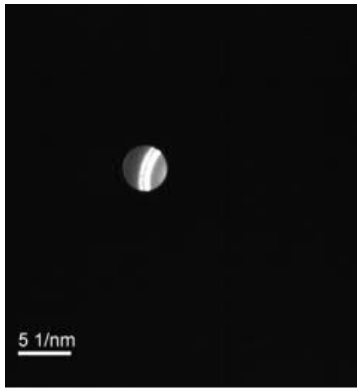

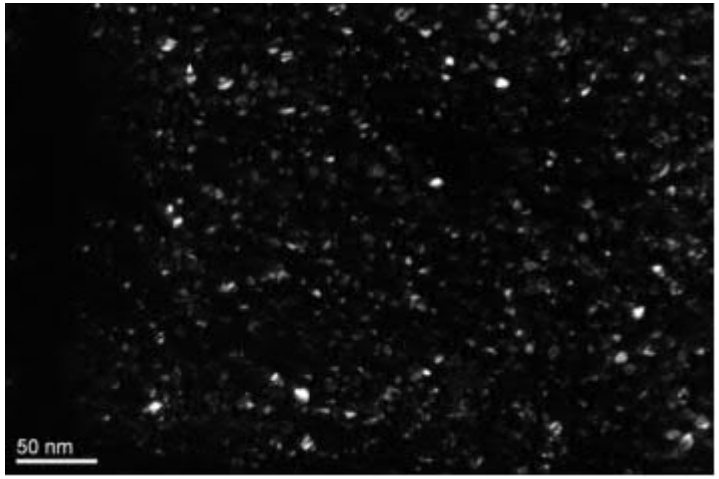

Dark Field

Two-Beam Condition - CDF

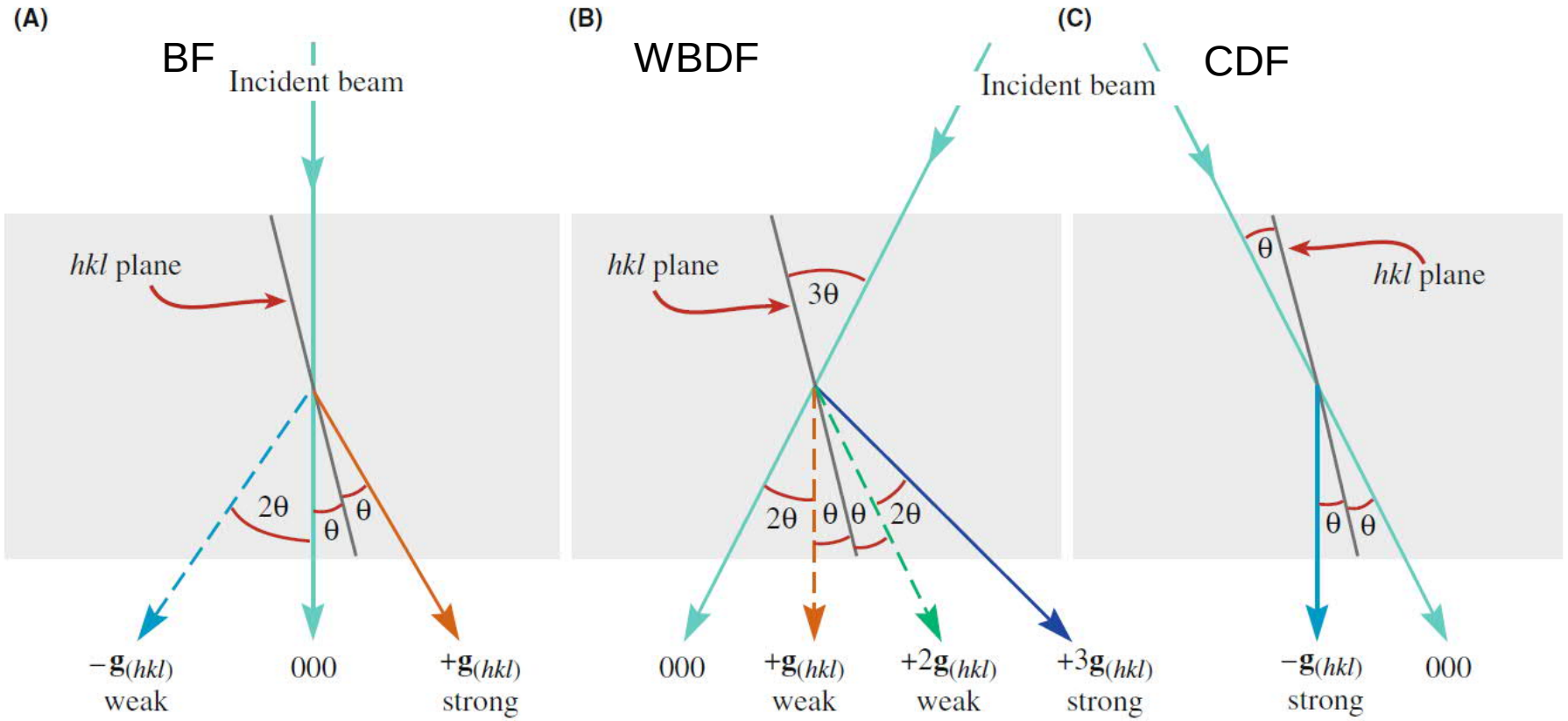

FIGURE 22.18. (A) Standard two-beam conditions involve the 000 spot and the *hkl* spot bright because one set of *hkl* planes are exactly at the Bragg condition. (B) When the incident beam is tilted through 2θ so that the excited $\mathbf{g}_{hkl}$ spot moves onto the optic axis, the $\mathbf{g}_{hkl}$ intensity decreases because the $\mathbf{g}_{3h3k3l}$ spot becomes strongly excited. (C) To get a strong *hkl* spot on axis for a CDF image, it is necessary to set up a strong $-\mathbf{g}_{hkl}$ condition first of all, then tilt the initially weak $\mathbf{g}_{hkl}$ maximum onto the axis.

The Origin of Thickness Fringes and Bend Contours – two beam condition

$$I_{\mathbf{g}} = |\phi_{\mathbf{g}}|^2 = \left(\frac{\pi t}{\xi_{\mathbf{g}}}\right)^2 \cdot \frac{\sin^2(\pi t s_{\mathrm{eff}})}{(\pi t s_{\mathrm{eff}})^2} = 1 - I_{\mathbf{0}} \qquad s_{\mathrm{eff}} = \sqrt{s^2 + \frac{1}{\xi_{\mathbf{g}}^2}}$$

$$\xi_{\mathbf{g}} = \frac{\pi V_{\mathrm{c}} \cos\theta_{\mathrm{B}}}{\lambda F_{\mathbf{g}}}$$

s_{eff} effective excitation error ξ_g extinction distance

The diffracted intensity is **periodic** in the two independent quantities, ***t*** and ***s_{eff}***. If we imaging the situation where *t* remains constant but *s* (and hence s_{eff}) varies locally, then we produce bend contours. Similarly, if *s* remains constant while *t* varies, then thickness fringes will result.

Thickness Fringes

Intensity of both the **0** and **g** beams oscillate as *t* varies. Furthermore, these oscillations are complementary for the DF and BF images.

- As a rule of thumb, when other diffracted beams are present the effective extinction distance is reduced.
- At greater thicknesses, absorption occurs and the contrast is reduced.

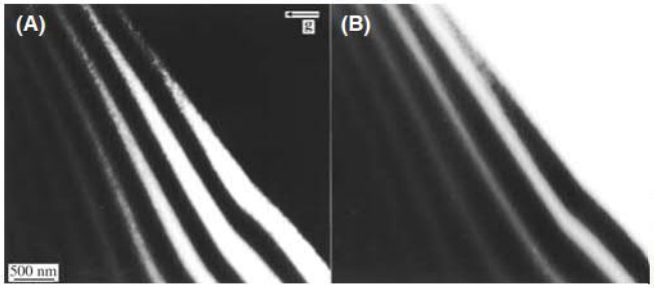

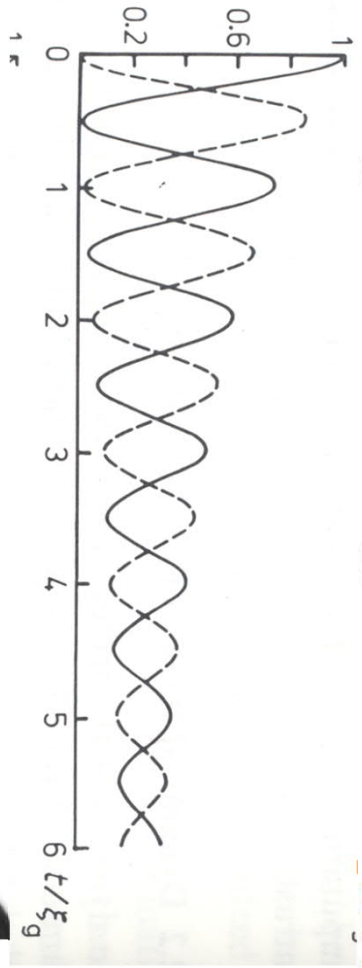

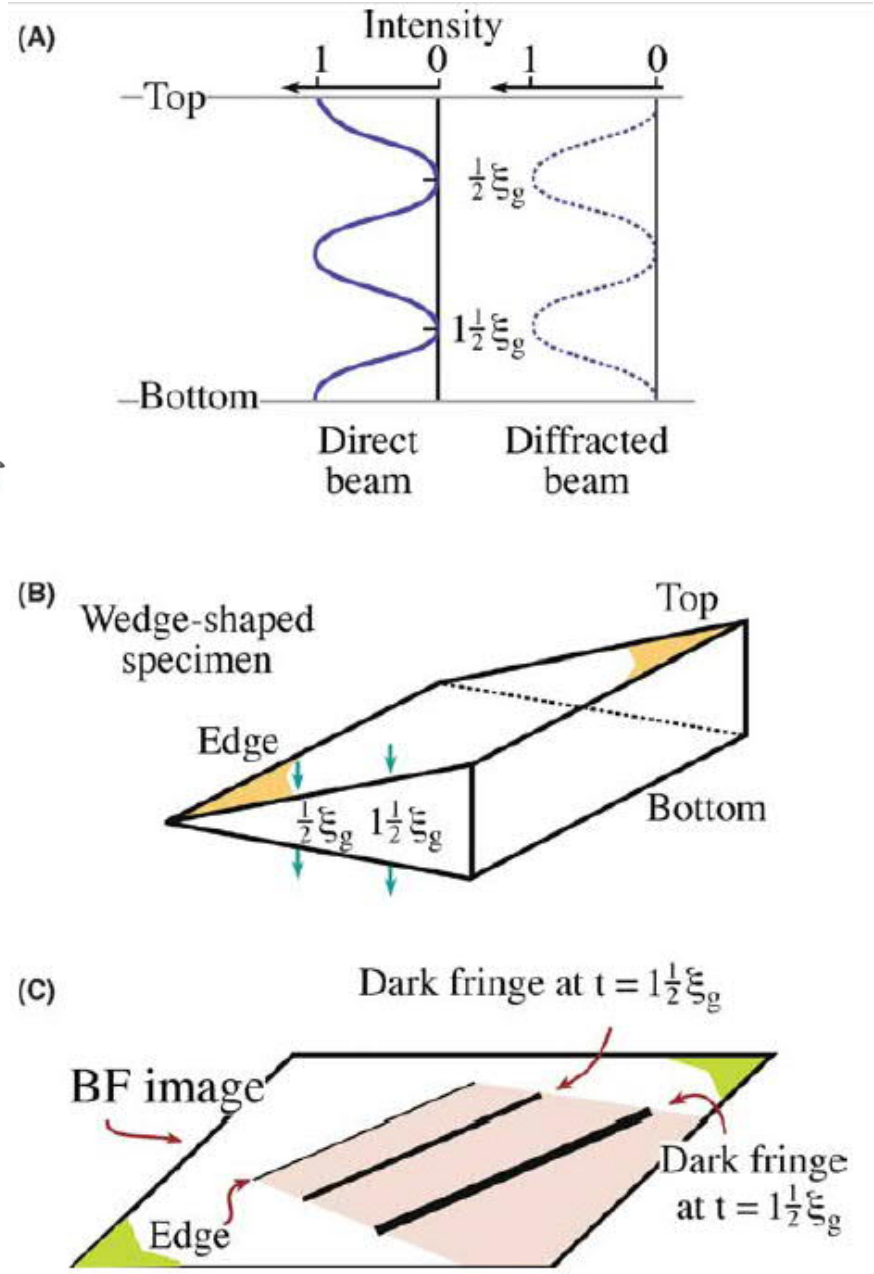

FIGURE 24.2. (A) At the Bragg condition (s = 0), the intensities of the direct and diffracted beams oscillate in a complementary way. (B) For a wedge specimen, the separation of the fringes in the image (C) is then determined by the angle of the wedge and the extinction distance, ξ_g.

Bend Contours (Annoying Artifact, Useful Tool, Invaluable Insight)

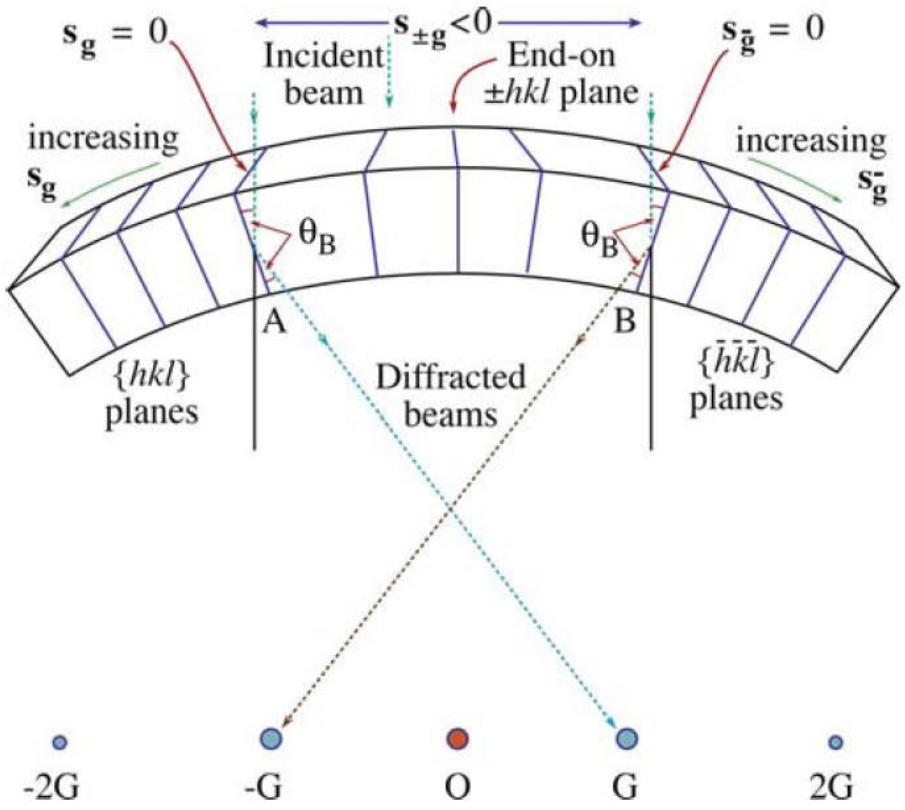

FIGURE 24.7. The origin of bend contours shown for a foil symmetrically bent either side of the Bragg conditions. For this geometry, when the *hkl* planes are in the Bragg condition, the reflection G is excited. Notice that G and the diffracting region are on opposite sides of O; if the foil were bent upwards, they would be on the same side.

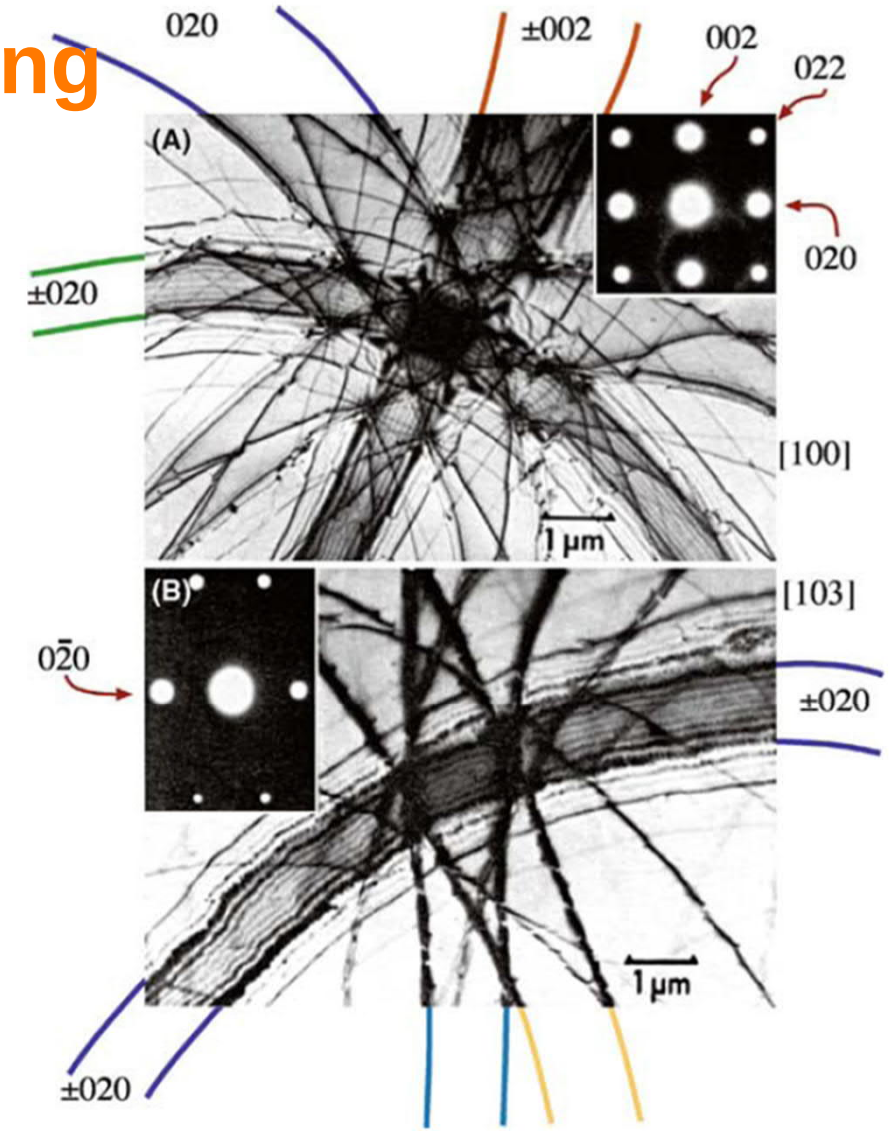

FIGURE 24.8. BF images of a bent Al specimen oriented close to the (A) [100] and (B) [013] zone axes. These images are known as (real-space) zone-axis patterns, or ZAPs, and are shown with their respective zone-axis DPs (insets). Each diffracting plane produces two bend contours, depending on whether θ_B or $-\theta_B$ is satisfied. Note that the separation of the bend contours is not uniform for any particular pair of planes because the curvature of the bending is not, in general, the same.

Planar Defects
- internal interfaces

$$\frac{d\phi_{\mathbf{0}(\mathrm{sub})}}{dz} = \frac{\pi i}{\xi_{\mathbf{g}}}\phi_{\mathbf{g}(\mathrm{sub})}\exp(2\pi i\mathbf{g}\,.\,\mathbf{R})$$

$$\frac{d\phi_{\mathbf{g}(\mathrm{sub})}}{dz} = \frac{\pi i}{\xi_{\mathbf{g}}}\phi_{\mathbf{0}(\mathrm{sub})}\exp(-2\pi i\mathbf{g}\,.\,\mathbf{R}) + 2\pi i s\phi_{\mathbf{g}}$$

$$\alpha = 2\pi\mathbf{g}\,.\,\mathbf{R}$$

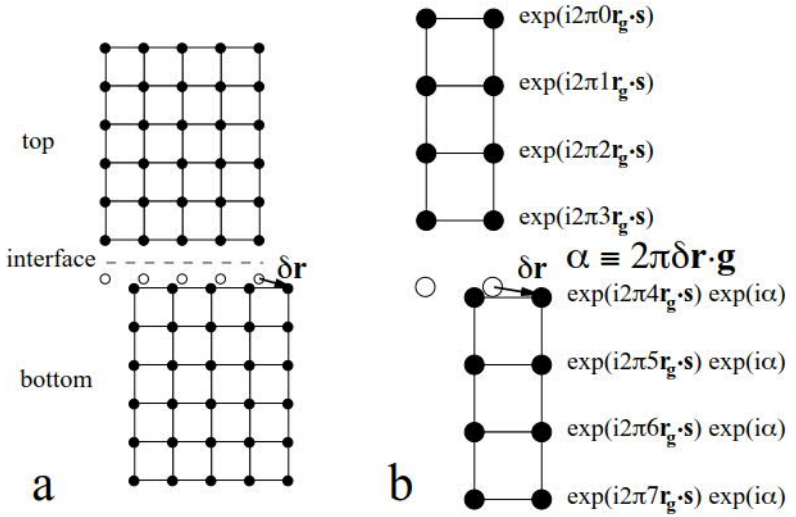

Fig. 7.43. (**a**) Example of a perfect crystal with an interface. Without the interface, the white circles indicate the positions of the next atoms from the top part of the crystal. The displacement across the interface is $\boldsymbol{\delta r}$. (**b**) A vertical column of unit cells in the vicinity of the interface, with phase factors as obtained in (7.40).

Visible: $\alpha \neq 0\ (\neq 2n\pi)$

Invisible: $\alpha = 0\ (= 2n\pi)$ -> g.R = integer

Brent Fultz , James M. Howe , Transmission Electron Microscopy and Diffractometry of Materials, Springer-Verlag Berlin Heidelberg, 10.1007/978-3-642-29761-8

Invisibility Criterion: $g \cdot R = 0,1,2\ldots$

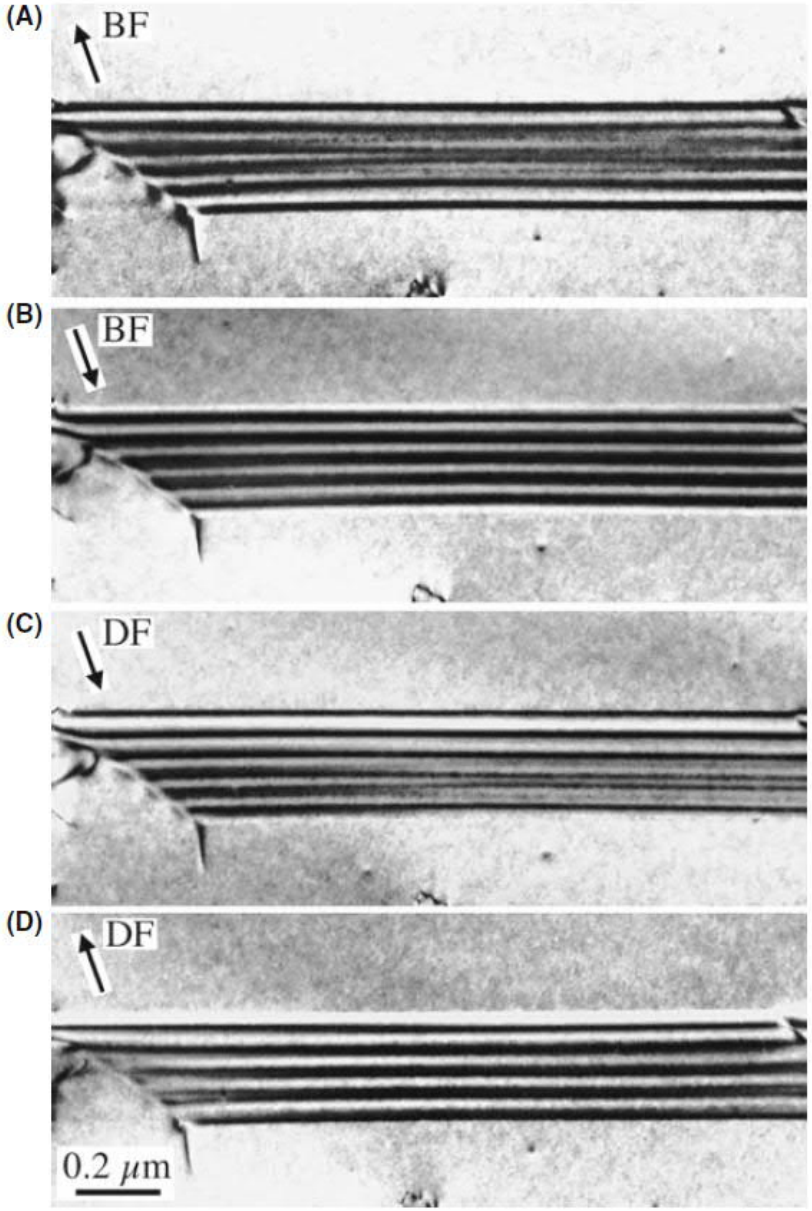

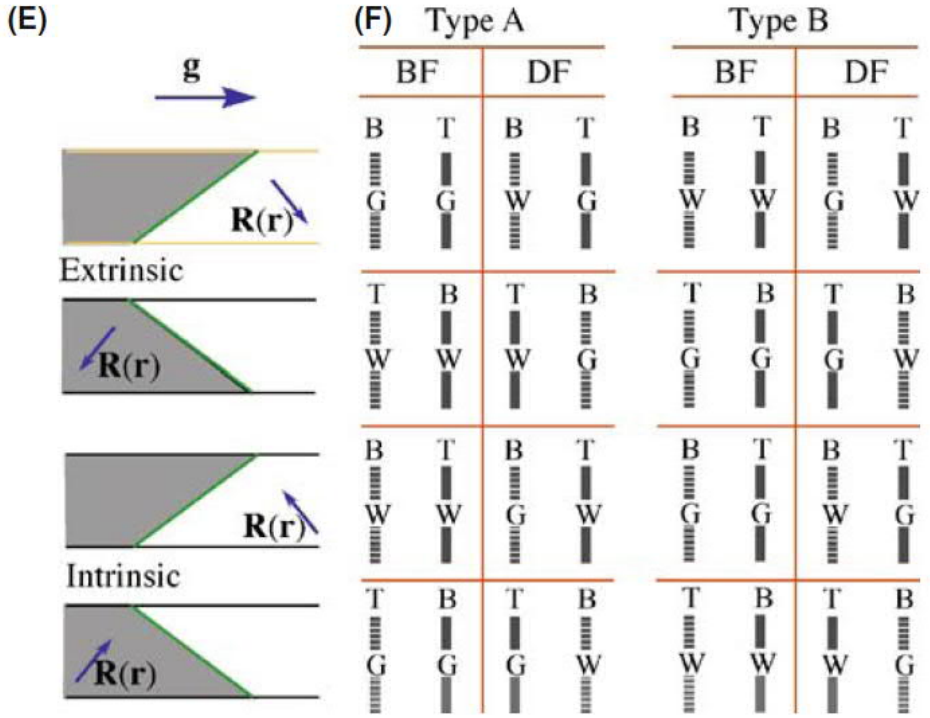

FIGURE 25.4. (A–D) Four strong-beam images of an SF recorded using ±g BF and ±g DF. The beam was nearly normal to the surfaces; the SF-fringe intensity is similar at the top surface but complementary at the bottom surface. The rules are summarized in (E) and (F) where G and W indicate that the first fringe is gray or white; (T, B) indicates top/bottom.

Invisible: g.R = 0 equal g.R =1 or integer $\alpha=2n\pi$ Visible: g.R =1/3 equal g.R = 4/3, |g.R| is 0 to 1.

Imaging Strain Field

- The direction and magnitude of the **Burgers vector, b**, which is normal to the *hkl* diffraction planes.
- **The line direction, u** (a vector), and therefore, the character of the dislocations (edge, screw, or mixed).
- **The glide plane**: the plane that contains both **b** and **u**.

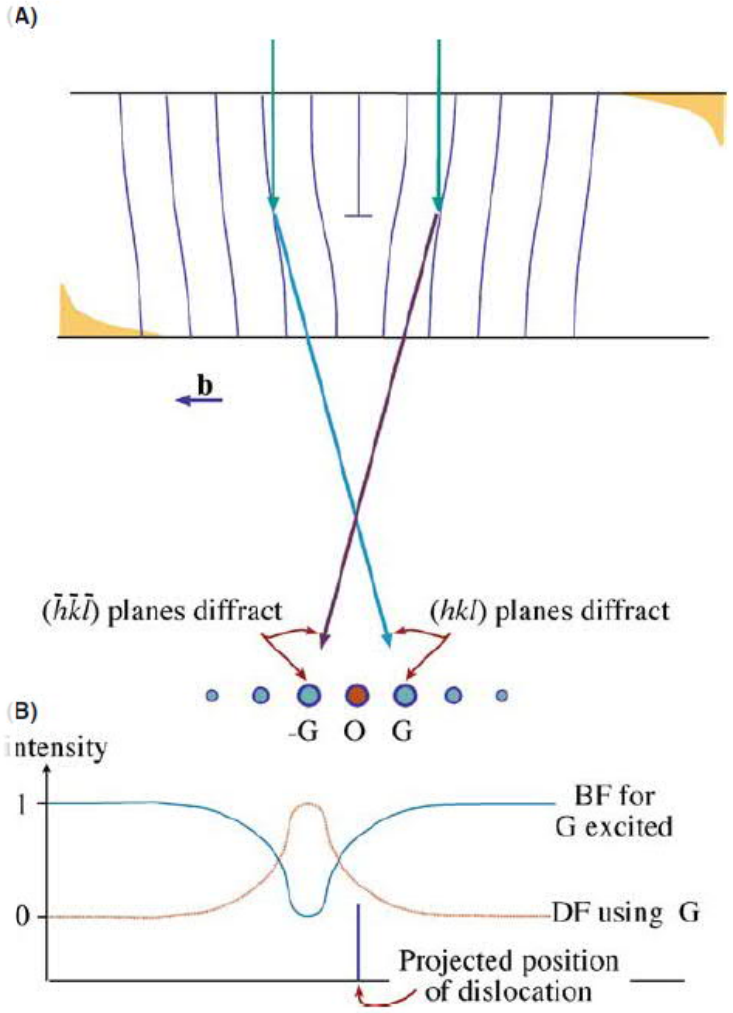

FIGURE 26.1. (A) The specimen is tilted slightly away from the Bragg condition ($s \neq 0$). The distorted planes close to the edge dislocation are bent back into the Bragg-diffracting condition ($s = 0$), diffracting into G and –G as shown. (B) Schematic profiles across the dislocation image showing that the defect contrast is displaced from the projected position of the defect. (As usual for an edge dislocation, **u** points into the paper.)

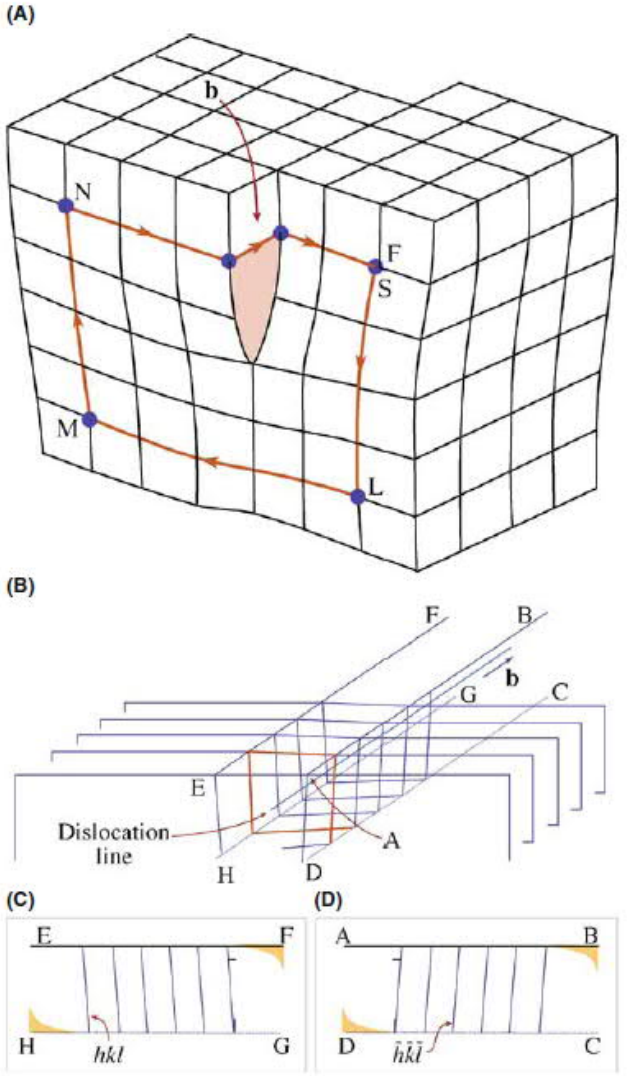

FIGURE 26.2. (A) Distortion of planes around a screw dislocation. The circuit SLMNF is used to define the Burgers vector, **b** (see Figure 26.5). (B) Schematic showing the rotation of the diffracting planes by a screw dislocation. The planes are rotated in opposite directions on either side of the dislocation. (C) and (D) show sections (ABCD and EFGH) through these diffraction planes.

g.b rule of dislocation

Screw dislocation invisible: *g* is perpendicular to ***b***

$$\mathbf{g} \cdot \mathbf{b} = 0$$

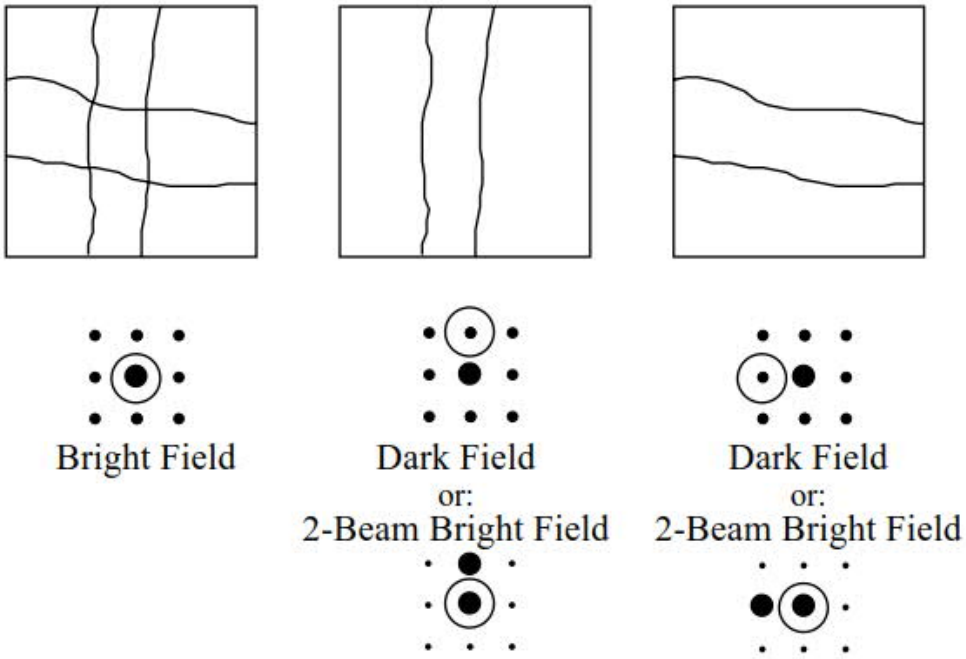

Fig. 7.24. Schematic diffraction contrast of screw dislocations.

g.b rule of dislocation

Edge dislocation invisible: g is perpendicular to $\boldsymbol{b}$ and g is in glide plane, g and $\boldsymbol{b}$ and $\boldsymbol{u}$ in sample plane

$$\mathbf{g}\cdot\mathbf{b}=0 \qquad \mathbf{g}\cdot(\mathbf{b}\times\mathbf{u})=0$$

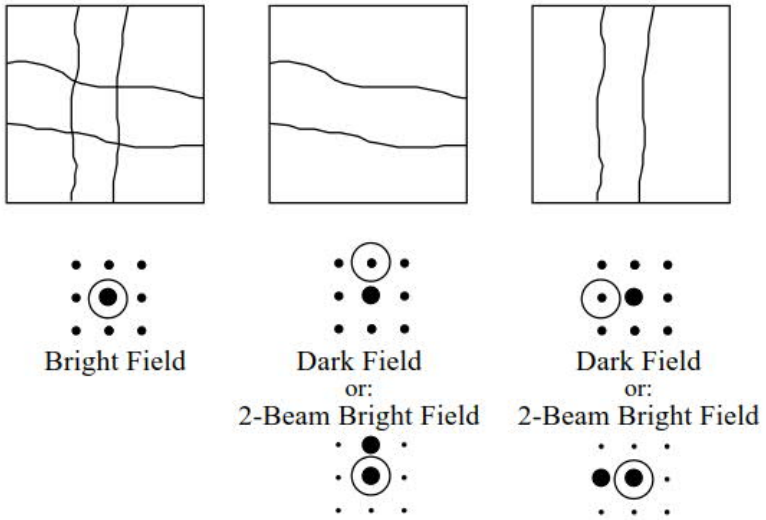

Fig. 7.20. Schematic diffraction contrast from edge dislocations with lines and $\boldsymbol{b}$ in the plane of the sample.

Example of determination of b

Table 7.1 *Possible values of* $\mathbf{g}\cdot\mathbf{b}$ *for the three dislocations under the reflections in Figure 7.27.*

g	½[110]	½[101]	½[011]	½[1$\bar{1}$0]	½[10$\bar{1}$]	½[01$\bar{1}$]	No. 1	No. 2	No. 3
13$\bar{1}$	2	0	1	−1	1	2	Inv.	Vis.	Vis.
040	2	0	2	−2	0	2	Inv.	Vis.	Vis.
1$\bar{1}$3	0	2	1	1	−1	−2	Vis.	Inv.	Vis.
00$\bar{4}$	0	−2	−2	0	2	2	Vis.	Inv.	Vis.
044	2	2	4	−2	−2	0	Vis.	Vis.	Inv.

Note: From inspection of this table the only consistent values for the Burgers vectors for the dislocations are those given in Figure 7.27.

Example: Analysis of dislocations in $MgAl_2O_4$ spinel

Figure 7.27 shows a series of bright field images of three intersecting dislocations, labelled 1, 2 and 3. By changing the orientation of the crystal, different planes can be put into the diffraction condition. The strongly diffracting planes in each case are specified by the reciprocal lattice vector **g** on each micrograph. In each case one of the dislocations is invisible and hence $\mathbf{g}\cdot\mathbf{b} = 0$. Since the shortest lattice vector in a face-centred cubic structure has the general form ½<110>, the analysis involves determining all possible $\mathbf{g}\cdot\mathbf{b}$ values and comparing these with the contrast observed for each dislocation. This is summarized in Table 7.1.

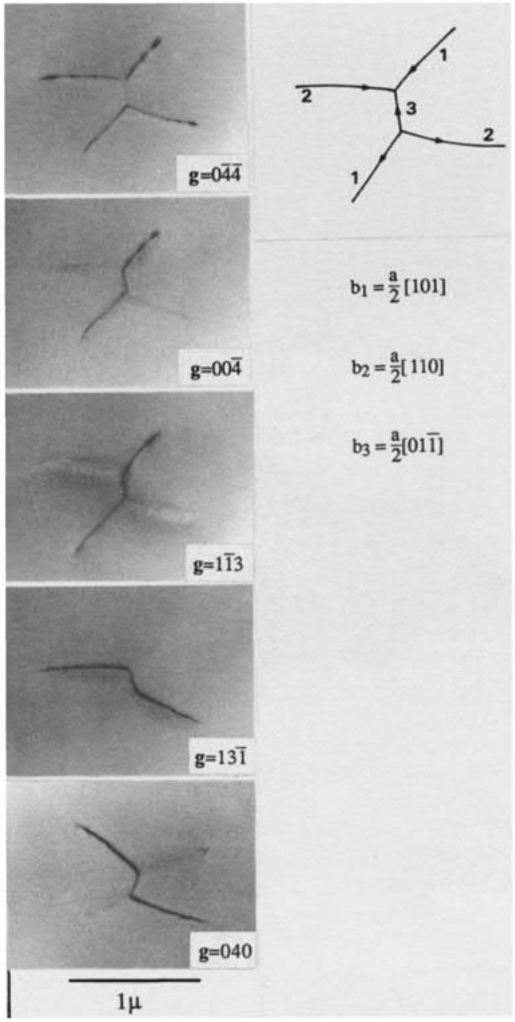

Figure 7.27. A series of electron micrographs of three intersecting dislocations (labelled 1,2,3) in spinel, illustrating the visibility/invisibility of the different dislocations when viewed under various diffracting conditions. The operative strongly diffracting beam, defined by the reciprocal lattice vector **g** is marked on each micrograph. Using the $\mathbf{g}\cdot\mathbf{b}$ criteria the Burgers vector for each dislocation can be determined. (Micrographs courtesy of C. Willaime.)

From book: **An Introduction to Mineral Sciences**

Phase Contrast HRTEM

The Origin of Lattice Fringes – phase contrast

Two beam condition, interference of direction beam and diffracted beam.

$$\mathbf{k}_D = \mathbf{k}_I + \mathbf{g} + \mathbf{s}_g = \mathbf{k}_I + \mathbf{g}'$$

$$I = A^2 + B^2 - 2AB\sin(2\pi g' x - \pi s t)$$

The intensity of phase contrast is a **sinusoidal oscillation** normal to ***g***', with a periodicity that depends on s and t.

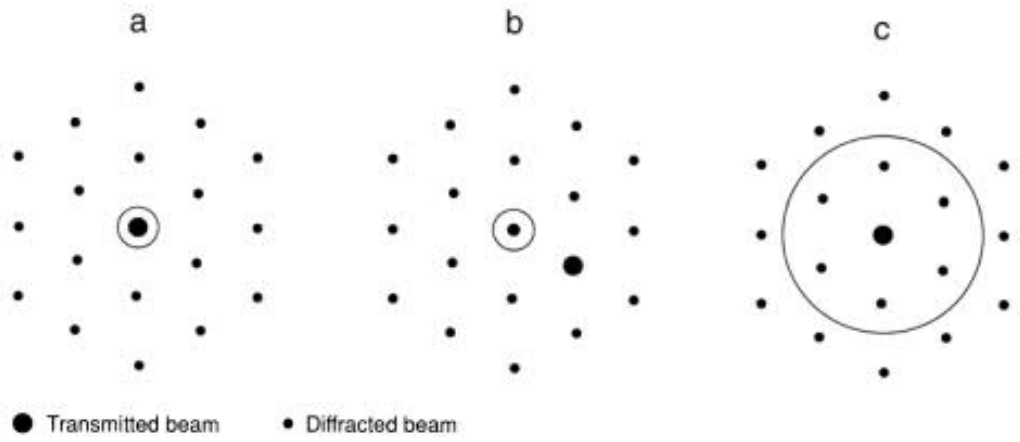

Fig. 1.2. Three observation modes in electron microscopy using an objective aperture. The center of the objective aperture is assumed to be set to the optical axis. **a** Bright-field method; **b** dark-field method; **c** high-resolution electron microscopy (axial illumination)

Image ≠ Real Structure

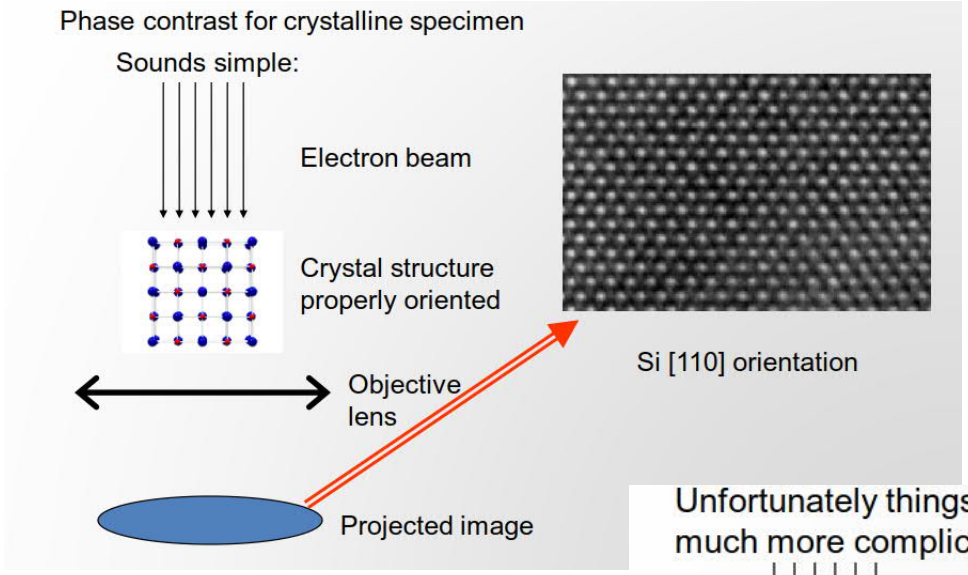

Ideal

Reality

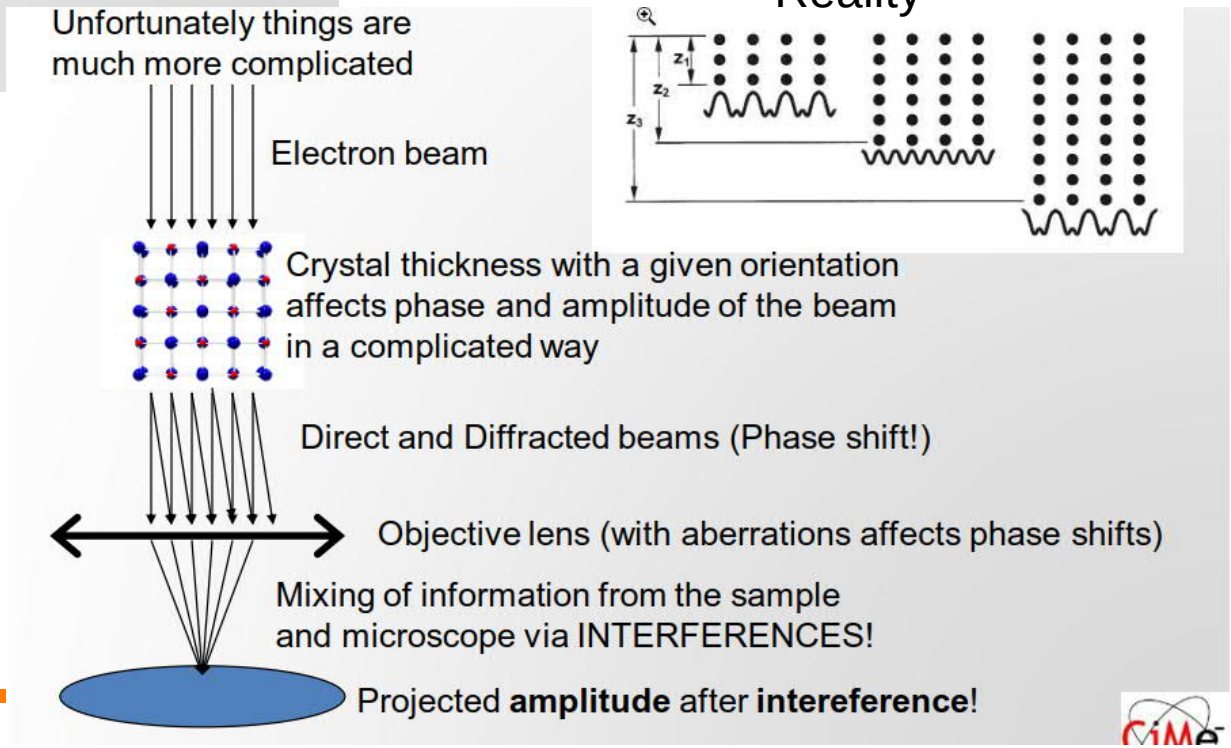

Formation of HRTEM

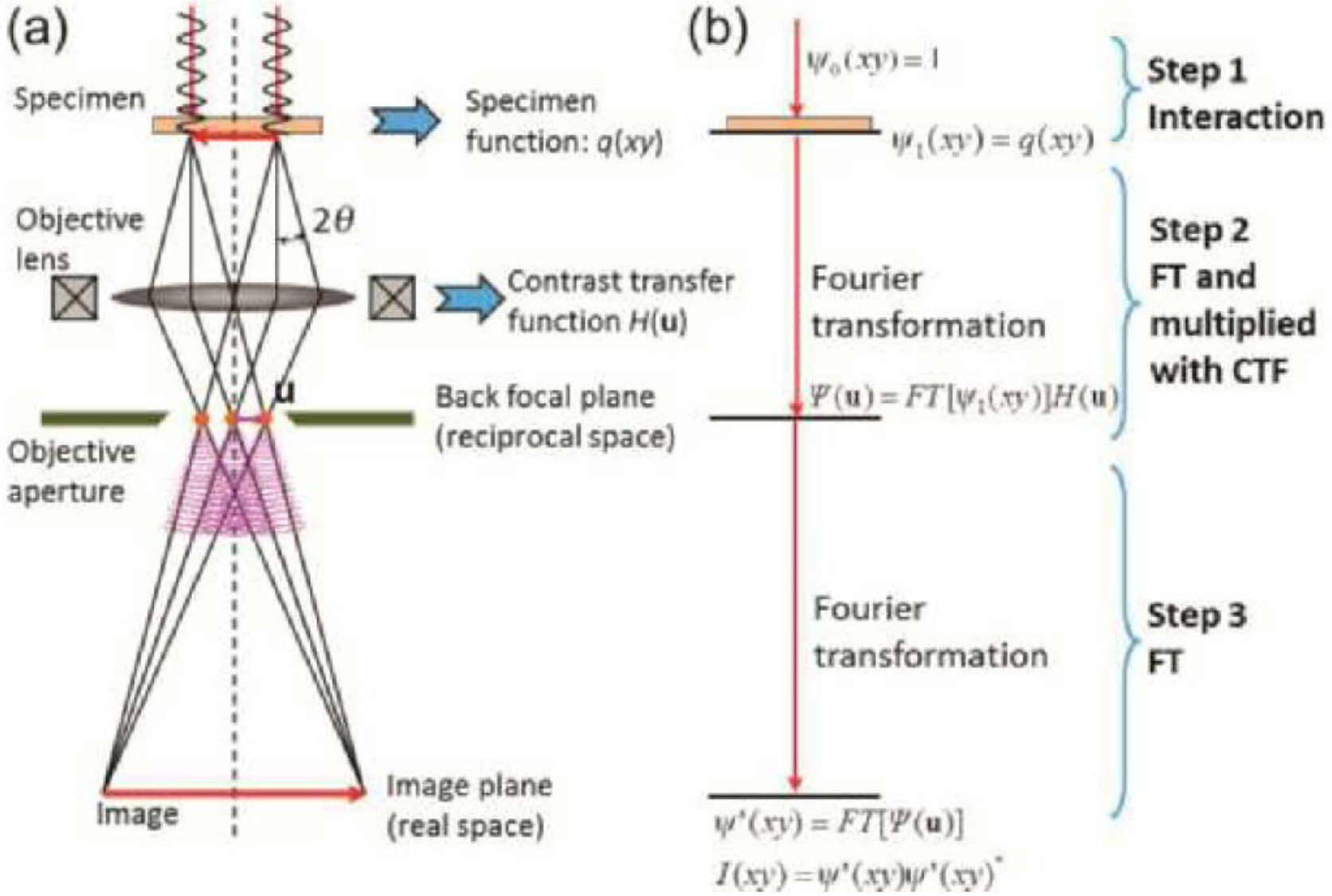

Fig. 7.6 Formation of HRTEM image. (a) Schematic imaging process in TEM; (b) mathematical processing.

Scherzer Defocus

Scherzer found that the CTF could be optimized by balancing the effect of spherical aberration against a particular negative value of Δf. this value has come to be known as Scherzer defocus, Δf_{Sch} which occurs at

$$\Delta f_{\mathrm{Sch}} = -1.2(C_s\lambda)^{1/2}$$

$$u_{\mathrm{Sch}} = 1.51 C_s^{-\frac{1}{4}} \lambda^{-\frac{3}{4}}$$

Scherzer resolution:

$$r_{\mathrm{Sch}} = \frac{1}{1.51} C_s^{\frac{1}{4}} \lambda^{\frac{3}{4}} = 0.66 C_s^{\frac{1}{4}} \lambda^{\frac{3}{4}}$$

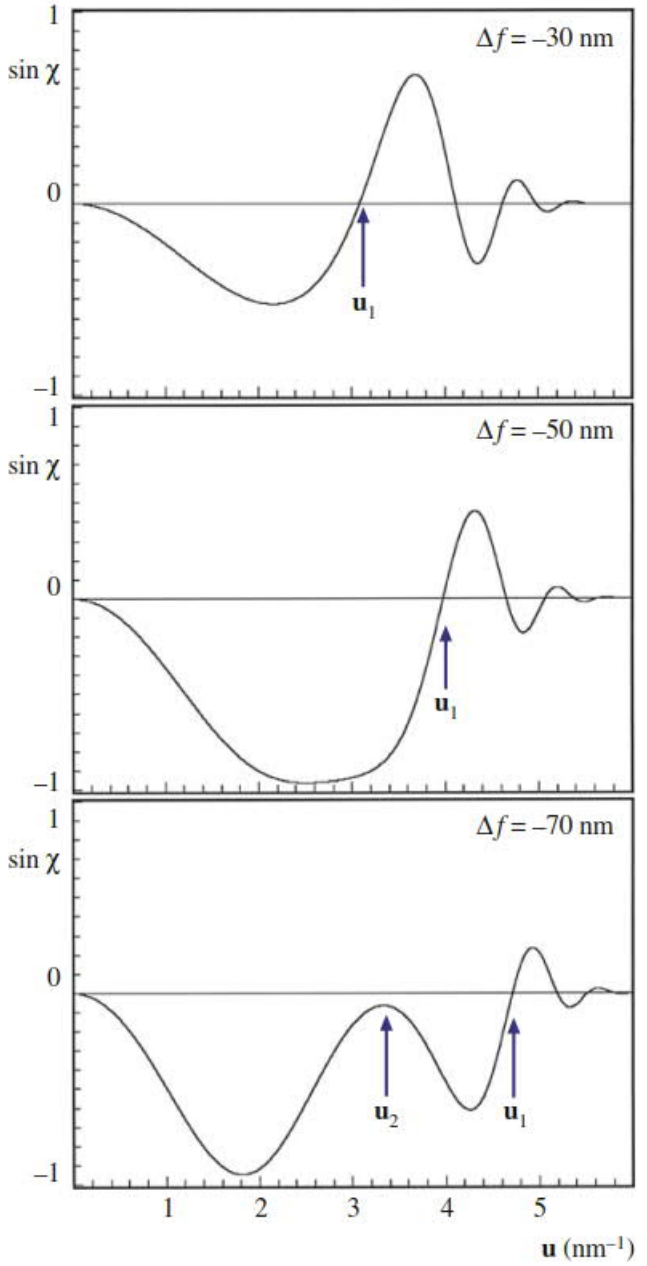

FIGURE 28.6. A series of sin χ curves calculated for different values of Δf. (E_0 = 200 kV; C_s = 1.0 mm.)

HRTEM example

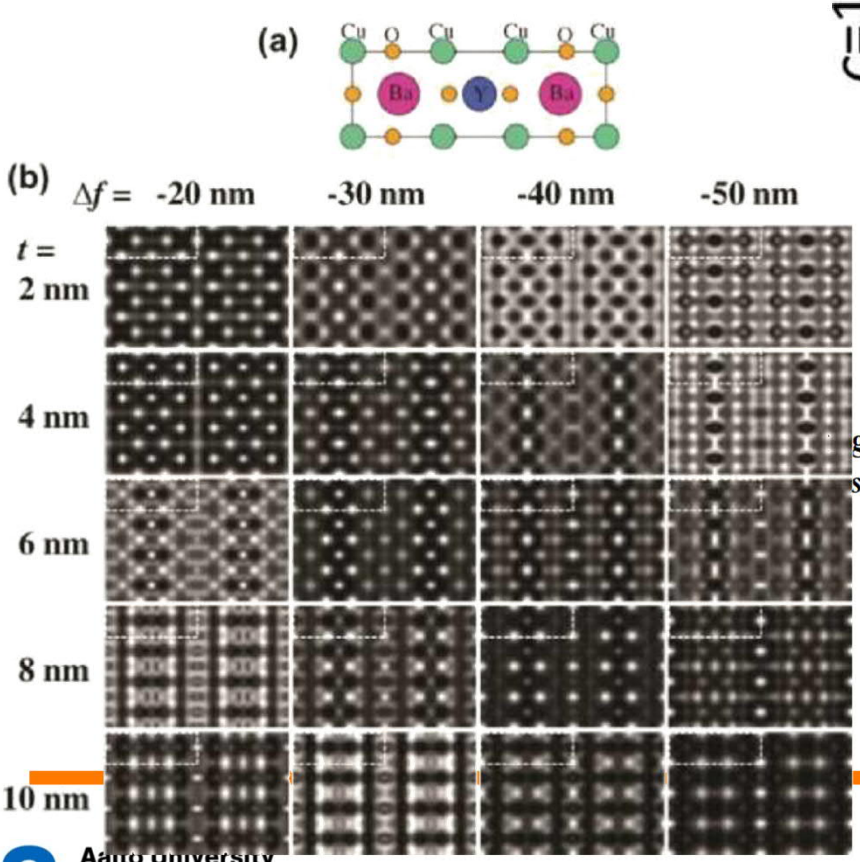

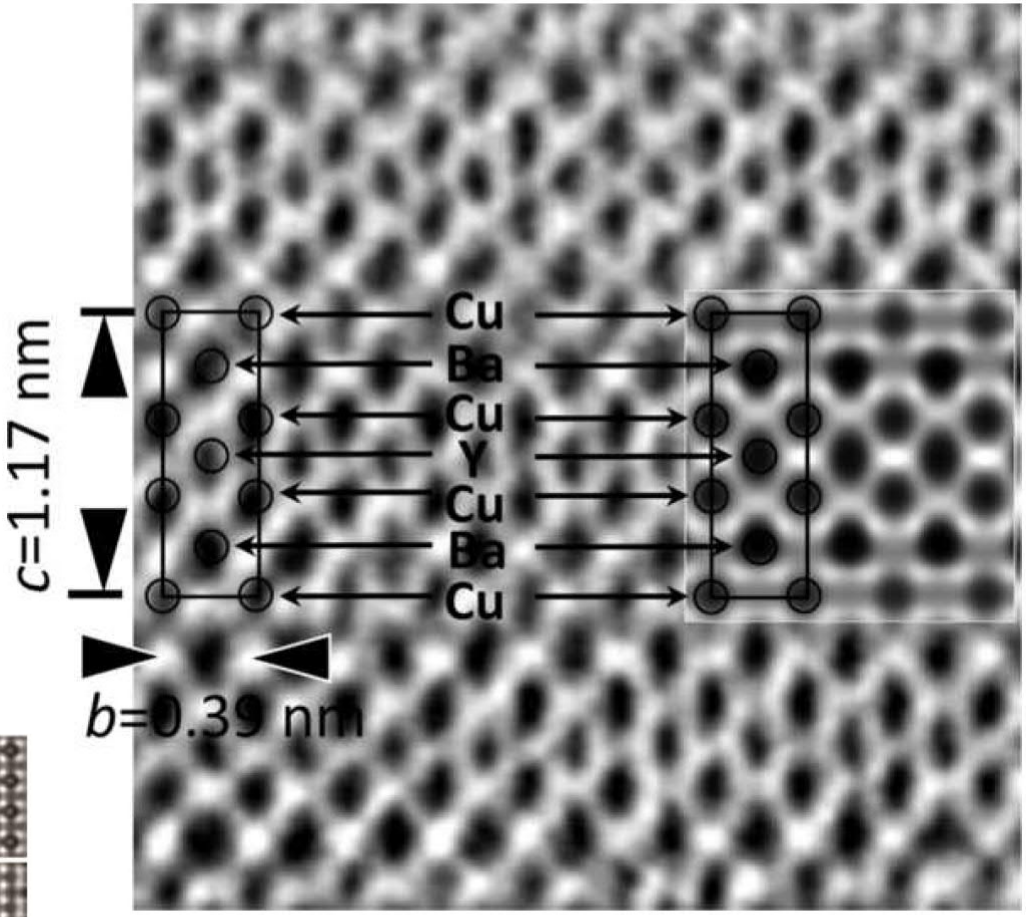

g. 7.16 *Experimental HRTEM image of YBCO compared with an serted image simulation.*

400kV, ∇f=-45nm

Specimen Preparation

Goal of TEM specimen

Electron transparency and representative of material you want to study

Safety: be aware of the hazard of using chemicals

Self-supporting Disk or Use a Grid?

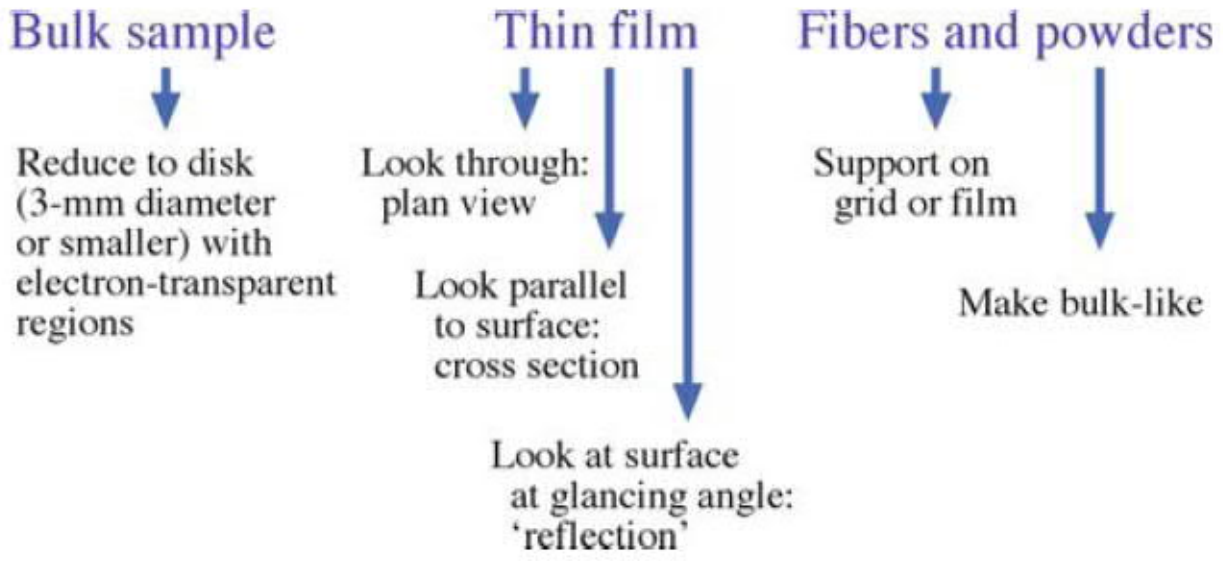

FIGURE 10.2. Flow chart summarizing the different sample geometries you may encounter.

Preparing a Self-Supporting Disk

Initial thinning to make a slice of material between 100 and 200 μm thick.	cutting and grinding.
Cut the 3-mm disk from the slice.	disk cutter using mechanical punch, or spark erosion, ultrasonic drilling and a grinding drill.
Pre-thin the central region from one or both faces of the disk to a few micrometers.	Dimpling mechanically or chemically
Final thinning of the Disks	Electropolishing, ion milling.

Cross-Section Specimens

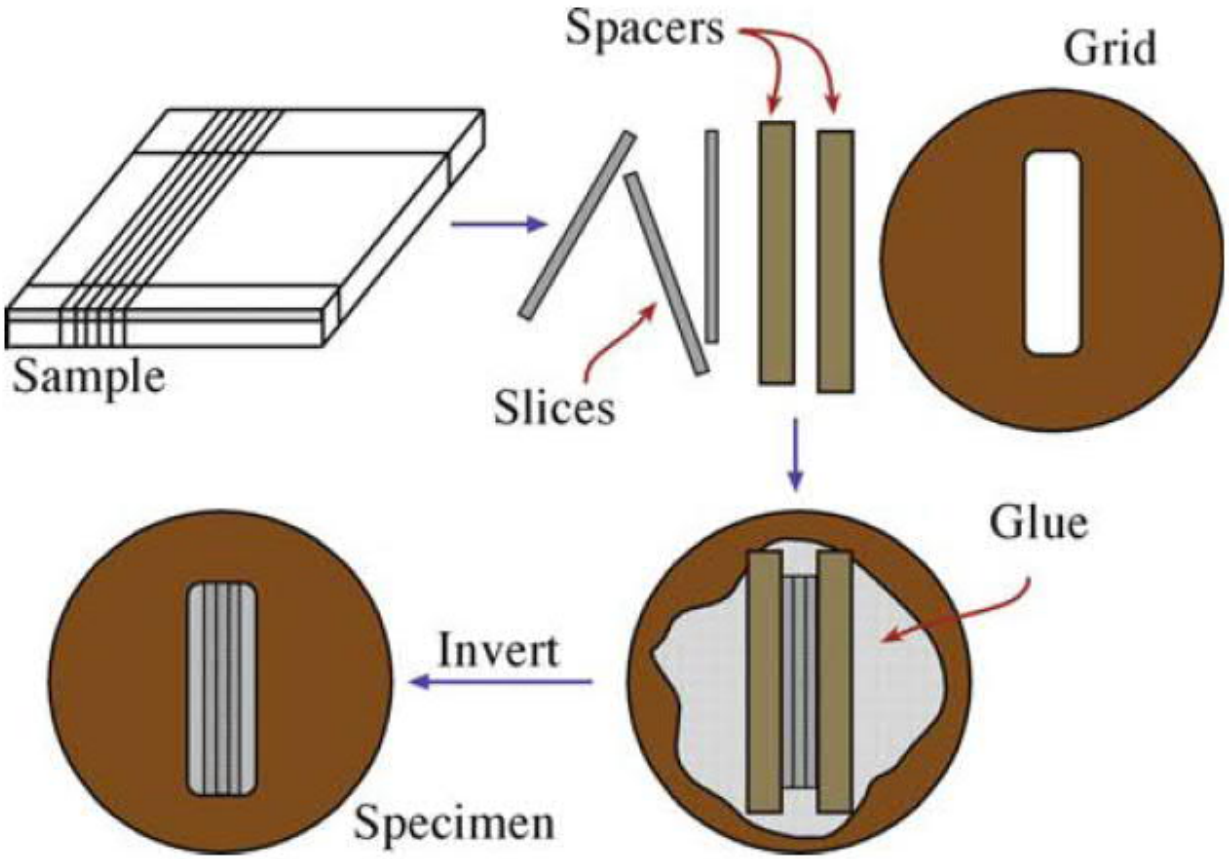

FIGURE 10.13. Schematic sequence for cross-section specimen preparation: the sample is cut into thin slices normal to the interfaces which are glued together between spacers which could be Si, glass, or some other inexpensive material so that they are wider than the slot in the grid. The 'club' sandwich is then itself glued to the grid (over the slot) and ion milled to perforation.

Specimens on Grids/Washers

- Electropolishing – the Window Method for Metals and Alloys
- Ultramicrotomy – biological materials
- Grinding and Crushing – ceramics and minerals
- Replication and Extraction – for study fracture surfaces or surface topography
- Cleaving and the SACT – graphite, mica and other layer materials
- The 90° Wedge – semiconductors
- Lithography – electronic materials
- Preferential Chemical Etching – III-V compounds
- FIB – any materials has good conductivity

References

[1] Z. Luo, A Practical Guide to Transmission Electron Microscopy: Fundamentals, Momentum Press, 2015. https://books.google.fi/books?id=ru8DCwAAQBAJ.
[2] C.B. Carter, D.B. Williams, Transmission Electron Microscopy: Diffraction, Imaging, and Spectrometry, Springer International Publishing, 2016. https://books.google.fi/books?id=jrnmDAAAQBAJ.
[3] R.F. Egerton, Physical Principles of Electron Microscopy: An Introduction to TEM, SEM, and AEM, Springer, 2016. https://books.google.fi/books?id=HhWfDAAAQBAJ
[4] B. Fultz, J.M. Howe, Transmission Electron Microscopy and Diffractometry of Materials, Springer Science & Business Media, 2012. https://books.google.fi/books?id=tgOC3vlEY0sC.
[5] https://cime.epfl.ch/MSE-637
[6] https://myscope.training/#
[7] https://cfamm.ucr.edu/manuals.html